

ELECTROPLATING OF CRYSTALLINE AND AMORPHOUS NICKEL-PHOSPHORUS COATINGS AND STUDY OF THEIR WEAR BEHAVIOUR

BY

MD. IFTIKHAR AHMED

A thesis submitted to the Department of Metallurgical Engineering Bangladesh University of Engineering and Technology, Dhaka in partial fulfillment of the requirements for the degree of Master of Science in Engineering (Metallurgical).



December, 1995

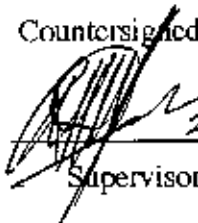
**BANGLADESH UNIVERSITY OF ENGINEERING AND TECHNOLOGY,
DHAKA, BANGLADESH**

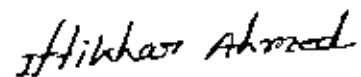


DECLARATION

This is to certify that this research work has been carried out by the author under the supervision of Dr. A.S.M.A. Haseeb, Assistant Professor, Department of Metallurgical Engineering, BUET, Dhaka and it has not been submitted elsewhere for the award of any other degree or diploma.


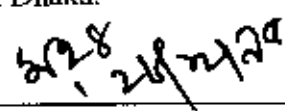
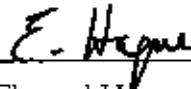
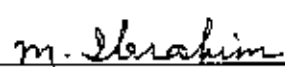
Countersigned


28/12/95
Supervisor



Signature of the author

The undersigned examiners appointed by the Committee of Advanced Studies and Research (CASR) hereby recommend to the Department of Metallurgical Engineering of Bangladesh University of Engineering and Technology, Dhaka, the acceptance of the thesis entitled "**ELECTROPLATING OF CRYSTALLINE AND AMORPHOUS NICKEL-PHOSPHORUS COATINGS AND STUDY OF THEIR WEAR BEHAVIOUR**" submitted by Md. Ifukhar Ahmed, B.Sc. Engg. (Metallurgical) in partial fulfillment of the requirements for the degree of Master of Science in Engineering (Metallurgical).

1. 
26/12/95
_____ Chairman
(Supervisor)
Dr. A.S.M.A. Haseeb
Assistant Professor
Department of Metallurgical Engg.
BUET, Dhaka.
2. 
28.12.95
_____ Member
(Ex-officio)
Head
Department of metallurgical Engg.
BUET, Dhaka.
3. 
_____ Member
Dr. Ehsanul Haque
Professor
Department of Metallurgical Engg.
BUET, Dhaka.
4. 
28.12.95
_____ Member
(External)
Professor M. Ibrahim
House No. 31, Road No. 4
Dhanmondi R/A, Dhaka.

ACKNOWLEDGEMENT

The author would like to express his gratitude and indebtedness to his thesis supervisor Dr. A. S. M. A. Haseeb, Assistant Professor, Department of Metallurgical Engineering, BUET, for his valuable suggestions, inspiring guidance, constant encouragement and kind help in carrying out the project and also in preparing this thesis.

The author is also indebted to Professor Md. Mohafizul Haque, Professor M. Ibrahim and Professor Ehsanul Haque of the Department of Metallurgical Engg. for their inspiration and suggestions in completing this thesis.

The author is grateful to Md. Ashikur Rahman, Laboratory Instructor, Md. Lutfur Rahman, Ex. Senior Crafts Instructor, Babu Binoy Bhushan Shaha, Senior Laboratory Instructor and other Laboratory Staff of Metallurgical Engg. Department of BUET for their kind help at different stages of this project.

Finally the author expresses his gratitude to well wishers for their encouragement and inspiration throughout the entire period of this undertaking.

**Dept. of Metallurgical Engg.
BUET, Dhaka-1000.**

The author

ABSTRACT

The electrolytic deposition of nickel-phosphorus coatings were carried out at various current densities (40 - 200 mA/cm²) in sodium hypophosphite based baths containing 150 g/l nickel sulphate, 45 g/l nickel chloride, 50 g/l phosphonic acid and various amount of sodium hypophosphite (5,75, 100 and 125 g/l) at a temperature of 60°C. The structure and composition of the coatings were determined by X-ray diffraction and chemical analysis respectively. Amount of sodium hypophosphite in the bath was found to have a pronounced effect on the character of the deposit. Bath containing 100 g/l was found to yield bright, compact and adherent deposits. All the deposits obtained at deposition current densities of 60, 100, and 200 mA/cm² from 100 g/l hypophosphite containing bath possessed a phosphorus content of about 14 wt%. X-ray diffraction pattern revealed these deposits to be amorphous. On the otherhand bath containing 5 g/l of hypophosphite yielded crystalline deposits.

Ni-P coatings were tested for thickness, microhardness and wear behaviour. The coating thickness was found to decrease with the amount of sodium hypophosphite in plating bath and increase with current density and deposition time. The microhardness of Ni-P coatings deposited at current densities of 60 mA/cm² and 100 mA/cm² were measured to be 701 VHN and 665 VHN respectively.

Using a pin-on-disc type apparatus under dry sliding conditions, wear behaviour of Ni-P coatings deposited at current densities of 60 and 100 mA/cm² on brass specimens was studied against gray cast iron counterbody. Wear experiments were done in the ambient air at room temperature under three different loads (180 g, 250 g and 480 g) for three sliding distances (416 m, 832 m and 1248 m) at a linear speed of 416 m/s. Extent of sliding wear damage was investigated by means of measurement of wear scar width and metallography. Ni-P coatings obtained at 100 mA/cm² was found to be more resistant to wear than Ni-P coatings deposited at 60 mA/cm². Both these coatings were found to possess wear resistance about four times higher than that of uncoated brass. Microscopic mechanism revealed that although abrasive wear mainly took place on Ni-P coatings, adhesive wear was also operative.

CONTENTS

DECLARATION

ACKNOWLEDGEMENT

ABSTRACT

1. INTRODUCTION	1
2. LITERATURE REVIEW	3
2.1 ELECTROPLATING OF CRYSTALLINE AND AMORPHOUS NICKEL-PHOSPHORUS ALLOY	3
2.2 MECHANISM OF NICKEL-PHOSPHORUS DEPOSITION	3
2.3 VARIABLES OF BATH COMPOSITION	6
2.3.1 Effect of Phosphite Concentration	8
2.3.2 Effect of Acid Concentration	10
2.4 VARIABLES OF BATH OPERATION	12
2.4.1 Effect of Current Density	13
2.4.2 Effect of Operating Temperature	17
2.4.3 Effect of Agitation	18
2.5 CURRENT DENSITY-POTENTIAL RELATIONS IN NICKEL-PHOSPHORUS ALLOY DEPOSITION	19
2.6 STRUCTURE AND PROPERTIES OF ELECTRODEPOSITED NICKEL-PHOSPHORUS ALLOY	21
2.6.1 Structure of Deposits	22
2.6.1.1 Microscopic Examination	22

2.6.1.2 X-ray Study	22
2.6.2 Physical and Mechanical Properties	24
2.6.2.1 Thickness	24
2.6.2.2 Hardness	26
2.6.2.3 Strength and Ductility	28
2.6.3 Electrical and Magnetic Properties	29
2.6.4 Density	30
2.6.5 Protective Value	31
2.6.6 Wear Resistance	32
3. EXPERIMENTAL	34
3.1 SUBSTRATE PREPARATION AND ELECTRODEPOSITION	34
3.1.1 Substrate Preparation	34
3.1.2 Electrodeposition Set-Up	35
3.1.3 Electroplating Operation	36
3.2 CHARACTERIZATION OF NICKEL-PHOSPHORUS COATINGS	38
3.2.1 Microhardness Measurement	38
3.2.2 X-Ray Diffraction	38
3.2.3 Chemical Analysis	39
3.3 WEAR TESTS AND EVALUATION	39
4. RESULTS AND DISCUSSION	41
4.1 COMPOSITION AND STRUCTURE	41
4.2 THICKNESS AND MICROHARDNESS	46
4.3 WEAR BEHAVIOUR	50
5. CONCLUSIONS	61
5.1 CONCLUSIONS DRAWN FROM THE PRESENT WORK	61
5.2 SUGGESTIONS FOR FURTHER WORK	62
6. REFERENCES	63

CHAPTER: ONE



1. INTRODUCTION

Nickel-phosphorus deposits were first produced in 1845 when Wurtz [1] observed that hypophosphite ions reduced nickel ions to nickel metal. In 1916 Roux [2] was granted a patent on the chemical deposition of nickel using hypophosphite ions as a reducing agent but the process attracted little attention until 1944.

The phosphorus alloys of nickel or cobalt were first deposited in the form of coherent coatings by the electroless plating process in 1947 developed by Brenner and Riddell [3]. This process is a chemical reduction of the metal salts with hypophosphite ion. The deposits were of considerable interest. They contained about 8% of phosphorus and were harder than ordinary electrodeposits of nickel or cobalt. They increased in hardness after being heat treated at 400°C and were not appreciably softened by heating to 600°C. They could be deposited dull or bright.

The properties of the electroless deposits were of sufficient interest to stimulate efforts to find more satisfactory conditions for depositing phosphorus alloys. Since the studies of Brenner and Riddell, much work has been conducted on electroless nickel solution and deposit properties. However, the use of nickel-phosphorus deposits has been restricted by the difficulties in the electroless plating process. As the process does not readily permit control of the phosphorus content of the deposits, Brenner et al. [4] developed an electrolytic process for depositing phosphorus alloys. These alloys are of both practical and theoretical interest.

Nickel-Phosphorus alloys are now-a-days recognized for their improved hardness, corrosion and wear resistance [5,6], interesting catalytic properties [7]. Consequently they are finding increasing applications in various industrial components in different

sectors including chemical, automotive, mining and electronics. Nickel-phosphorus coatings are also being considered for electrical connectors used in electronics, telecommunication and computer technology as a cheap replacement for the currently used gold coatings.

In the present study, electrodeposition of nickel-phosphorus coatings has been attempted from hypophosphite based baths. Deposited coatings have been characterized by chemical analysis and X-ray diffraction. Hardness and wear resistance of these coatings have been studied. Effect of process parameters on coating thickness, hardness and wear resistance have also been investigated.

CHAPTER: TWO

2. LITERATURE REVIEW

2.1 ELECTRODEPOSITION OF CRYSTALLINE AND AMORPHOUS NICKEL-PHOSPHORUS ALLOYS

One important feature of electrolytic Ni-P coatings is that by controlling the plating parameters and bath chemistry, crystalline or amorphous structures can be obtained to satisfy specific needs.

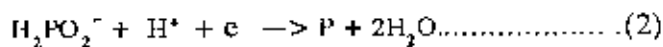
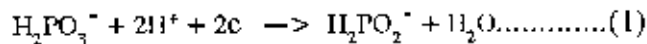
In general, it has been shown that if the amount of phosphorus dissolved in nickel exceeds about 12% then the structure of Ni-P alloys becomes amorphous[8]. Below this percentage of phosphorus, the alloy remain microcrystalline. This transition from the finely crystalline to the amorphous state is, however, not very well defined[9-11] and probably proceeds over a considerable range of concentration. Furthermore, as discussed recently else where[12], the critical concentration for the transition from ferromagnetism to paramagnetism in the Ni-P system also lies close to this composition.

2.2. MECHANISM of NICKEL-PHOSPHORUS ALLOYS DEPOSITION

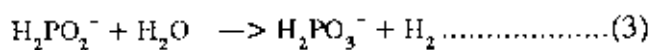
Brenner [13] studied two types of electrodeposition mechanism by which an ion in solution becomes a metal atom in a lattice. One of these which has been much discussed is whether the atom deposits at some random position and then diffuses into its final position. If atoms could migrate, one could expect them to take up equilibrium positions in the lattice, producing an alloy having the lowest energy content. However, many electrodeposited alloys are not in equilibrium and, hence, are metastable and posses more energy than the equilibrium alloy. If atoms could diffuse appreciably, they would not take up a metastable position.

Brenner [13] suggested that electrodeposition of nickel-phosphorus alloy is of the induced type. Induced codeposition is characterized by the deposition of alloys containing metals such as molybdenum, tungsten, phosphorus or germanium, which can not be deposited alone. However, these metals readily co-deposit with the iron group metals. Metals which stimulate deposition are called inducing metals and the metals which do not deposit by themselves are called reluctant metals. Thus phosphorus is the reluctant component while nickel is the inducing metal.

Two types reduction mechanism in the electrodeposition of Ni-P alloys are described in the literature. One is the direct reduction and other is indirect one. In a direct reduction mechanism for electrodeposition of Ni-P alloy proposed by Narayan et al. [15], phosphorus acid which is the supplier of P, is partly reduced to hypophosphite. This hypophosphite is further reduced to P, according to reactions (1) and (2).



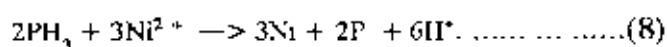
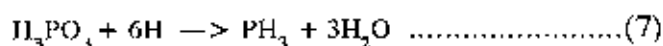
But hypophosphite (H_2PO_2^-) can also partly oxidize to phosphite (H_2PO_3^-) accompanied by excessive hydrogen evolution by a homogeneous reaction (3) at the anode, thereby decreasing the overall efficiency.



Furthermore, nickel and hydrogen ions can be reduced



An indirect mechanism for electrodeposition of Ni-P alloy has been proposed by Ratzker et al. [16] in the presence of Ni ions:



Carbajal et al. suggested that the direct reduction of hypophosphite (H_2PO_2^-) and nickel ions would be expected to produce a co-deposition of nickel and phosphorus with high P content in acid medium. On the other hand, the efficiency in the indirect reduction, according to reactions (6)-(8), with formation of phosphine (PH_3), as an intermediate from nascent hydrogen would be lower.

Phosphoric and phosphorus acid are suppliers of protons. These protons are consumed in the phosphite and hypophosphite reduction [Reactions (1) and (2)] and in the production of hydrogen. Electrodeposition of Ni-P is greatly reduced by the vigorous hydrogen evolution. However, the reduction of phosphite and hypophosphite according to reactions (1) and (2) require protons which are not available at the solution-cathode interface. This fact will drop the rate of deposition of P [14].

At high cathodic potentials, nickel is preferentially deposited over phosphorus. This suggests that codeposition of nickel and phosphorus continuous though the rate of phosphorus codeposition is slower. An increase in the number of moles of nickel in the solution with a fixed amount of phosphorus increased the amount of nickel in the deposited alloy. This is also valid for P i.e. increase of phosphite in solution increase the content of P in the alloy [14].

Since nickel electrocrystallization takes place in a face-centered cubic system (fcc) and the co-deposition of phosphorus takes place in the octahedron sites, the presence of phosphorus in the nickel crystal lattice would distort its structure, thus breaking the periodicity and producing an amorphous material [14].

Electroplated Ni film is crystalline, with a preferred orientation of 220. When 5% P is mixed into this Ni film, the orientation is changed to 111 and the crystals in the film assume an elliptical or columnar shape about 50\AA in diameter and 100\AA or less in length, perpendicular to the surface of the film. When the concentration of P reaches about 10%,

the crystals assume a needle shape, and at higher P concentration the needle length decreases and the film becomes amorphous [17].

2.3 VARIABLES OF BATH COMPOSITION

A typical bath for the electrodeposition of Ni-P coatings may have the following components:

- 1) Nickel source: mainly nickel sulfate ($\text{NiSO}_4 \cdot 6\text{H}_2\text{O}$) is used. In addition, nickel chloride ($\text{NiCl}_2 \cdot 6\text{H}_2\text{O}$) is also used in the bath.
- 2) Phosphorus source: either phosphorus acid (H_3PO_3) or sodium hypophosphite ($\text{NaH}_2\text{PO}_2 \cdot \text{H}_2\text{O}$) can be used. Phosphorus acid being cheaper, is commonly employed in electrodeposition of Ni-P alloys. Occasionally combination of both have also been employed. However phosphorus acid is not available in the local market. Present work therefore carried out using sodium hypophosphite.
- 3) Buffering agent: phosphoric acid (H_3PO_4) is used as buffering agent to control pH of the bath in order to avoid precipitation of basic nickel hydroxide. H_3BO_3 is sometime used as buffering agent.
- 4) Nickel carbonate (NiCO_3) has sometime been used as a neutralizing agent.

Information on the bath composition used by different researchers for the deposition of nickel-phosphorus alloys are summarized in Table 2.1. It is seen that the baths contain nickel sulfate (main source of nickel) within a narrow range viz, 150-170 g/l. Amount of nickel chloride in most of the baths is between 45-50 g/l. Ranges in the amount of phosphoric acid, phosphorus acid are quite wide.

Table 2.1 Summary of information on bath composition used by different researchers for the electrodeposition of nickel-phosphorus alloy

Bath Designation and Reference	NiSO ₄ ·6H ₂ O (g/l)	NiCl ₂ ·6H ₂ O (g/l)	NaH ₂ PO ₂ ·H ₂ O (g/l)	H ₃ PO ₃ (g/l)	H ₃ PO ₄ (g/l)	NiCO ₃ (g/l)	H ₃ BO ₃ (g/l)	pH
Bath A Ratzker et al [16]	150	45	—	50	40	45	—	0.77- 0.88
Bath B Rajagopal et al [26]	150	45	100	—	50	—	—	2
Bath C Husheng et al. [27]	170	20	<35	—	—	—	20	2.0
Bath D Brenner et al. [4]	175	50	—	1.3	50	—	—	0.5- 1.0
Bath E Brenner et al. [4]	150	45	—	40	50	—	—	0.5- 1.0
Bath F Atanasiu et al. [18]	150	50	—	40	200 ml	—	—	—
Bath G Bredael et al. [19]	150	50	—	3	42	—	—	1.0
Bath H Bredael et al. [19]	150	50	—	8	42	—	—	0.98
Bath I Bredael et al. [19]	150	50	—	27	42	—	—	0.75
Bath J Bredael et al. [19]	150	50	—	40	42	—	—	0.69
Bath K Bredael et al. [19]	150	50	—	55	42	—	—	0.60
Bath L Bredael et al. [19]	150	50	—	70	42	—	—	0.43
Bath M Toth Kadar et al [35]	160	45	—	40	40	28	—	1.0
Bath N Toth Kadar et al. [35]	163	45	—	35	40	26	—	1.0
Bath O Toth Kadar et al [35]	167	46	—	30	40	25	—	1.0
Bath P Toth Kadar et al [35]	171	46	—	25	40	22	—	1.0

2.3.1 Effect of Phosphite Concentration

The curves in Fig.2.1 represent typical relations between the composition of the deposit and the composition of the bath in induced codeposition [13].

Amount of phosphorus in the deposit increase as the amount of phosphorus in the bath increases. However, the rate of increase phosphorus in the deposit is not as high as that of tungsten in Fe-W alloy.

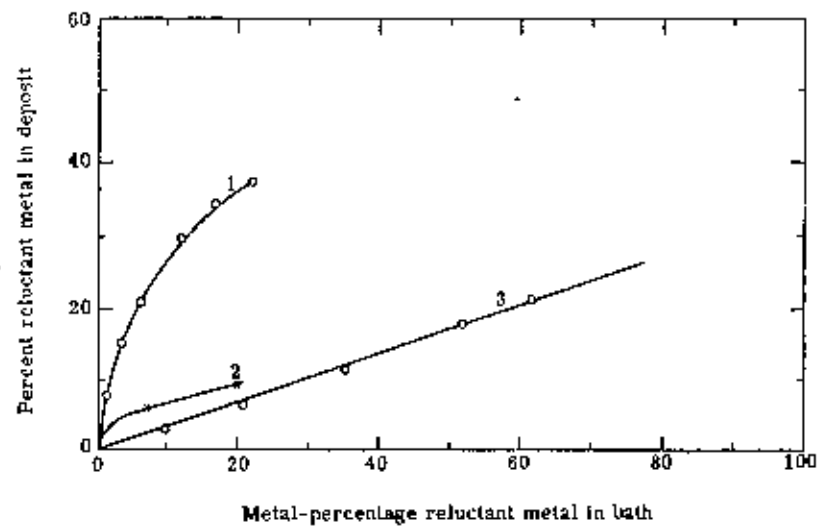


Fig. 2.1 Relation between composition of bath and composition of deposits in induced codeposition. The reluctant elements are tungsten, phosphorus and molybdenum [13] Curve 1, Tungsten-iron alloys deposited from acid solution. Curve 2, Phosphorus-nickel deposits from an acid bath. Curve 3, molybdenum-nickel alloys deposited from ammoniacal bath.

The phosphorus content of the nickel-phosphorus alloys varied with the concentration of phosphorus acid in the bath, as shown in Fig.2.2 [4, 18].

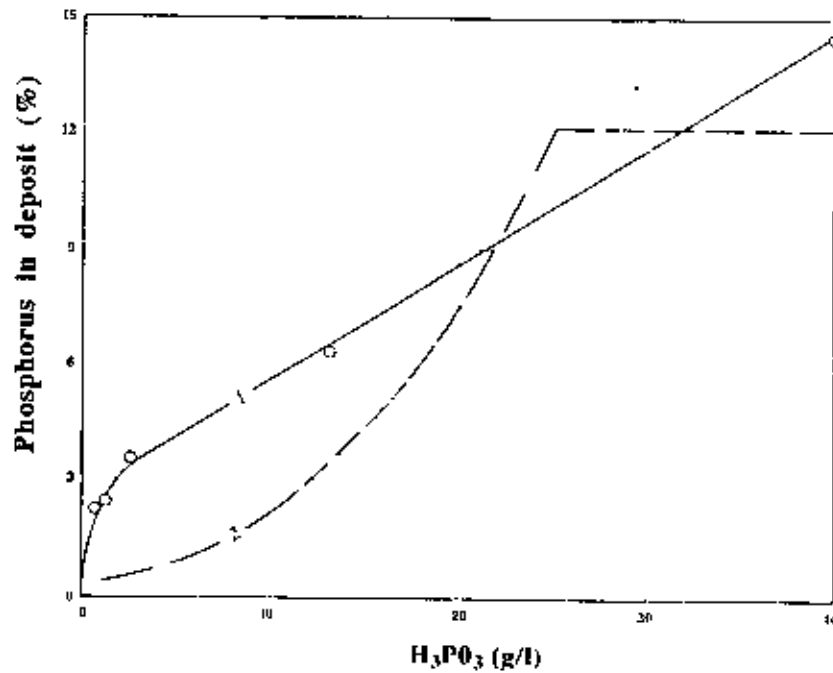


Fig. 2.2 Variation of the phosphorus content of electro-deposited nickel-phosphorus alloys with the phosphorus acid content of the bath. Curve 1 represent data of Brenner et al. [4]; Curve 2 data of Atanasiu and co-workers [18]. Bath operated at 75°C and 10 amp/dm²

Curve 1 is for nickel-phosphorus alloys deposited from bath E (see Table 2.1 for composition) Curve 2 shows data for nickel-phosphorus alloys deposited from bath F as given in Table 2.1 for composition. Both curves generally show an increase phosphorus content of the deposit as the amount of phosphorus acid in the bath increase. The largest content of phosphorus obtained by Brenner and co-workers in the nickel deposit was about 15%.

Bredael et al.[19] have also observed in a jet-cell that an increase in H₃PO₃ content in the electrolyte gives rise to a higher amount of phosphorus incorporated into the deposit (Fig.2.8).

As for cathode current efficiency, it was found [13] that current efficiency at the cathode decrease until deposition finally ceases as the metal percentage of the reluctant metal in the bath is increased [13]. In the case of nickel-phosphorus alloy deposition, relation between cathode current efficiency and amount of phosphorus acid in the bath is shown in Fig.2.3. The cathode current efficiency of deposition decreased markedly as the content of phosphorus acid in the bath was increased. The same effect may also be seen in Fig.2.10 by comparing curve 1 and 2 [4].

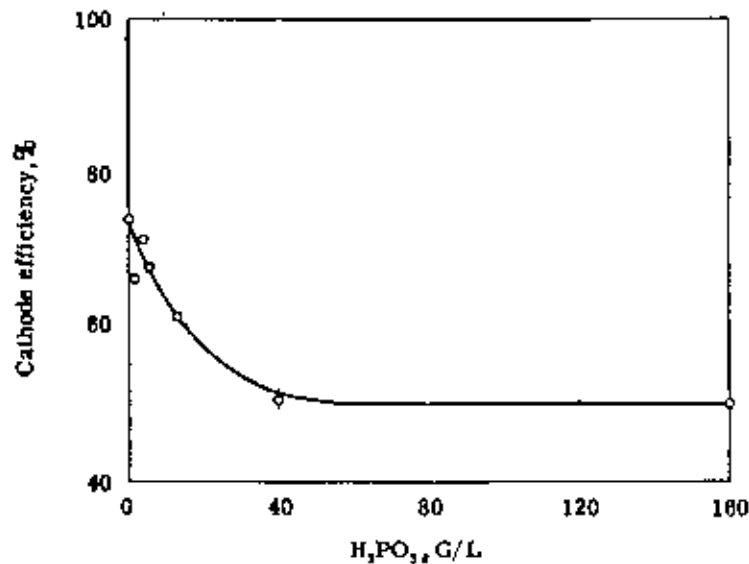


Fig. 2.3 Effect of concentration of phosphorus acid in the bath on the cathode current efficiency of deposition of phosphorus alloys. The curve represent data of Brenner et al.[4].

2.3.2 Effect of Acid Concentration

The effect of pH on the composition of alloys in induced type of codeposition is more complicated than on the other types of alloy systems [13].

Within the operable plating range of the moderately acid baths, Brenner et al. noted no appreciable effect of pH on the phosphorus content of the deposits. However, Atanasiu et al. [18] using baths of much higher phosphoric acid content, observed a decrease in the

phosphorus content of the deposit with increased acidity of the bath. Their data are shown in Fig. 2.4. The cathode current efficiency of deposition of the alloy decreased considerably with increase in the acidity of the bath [18].

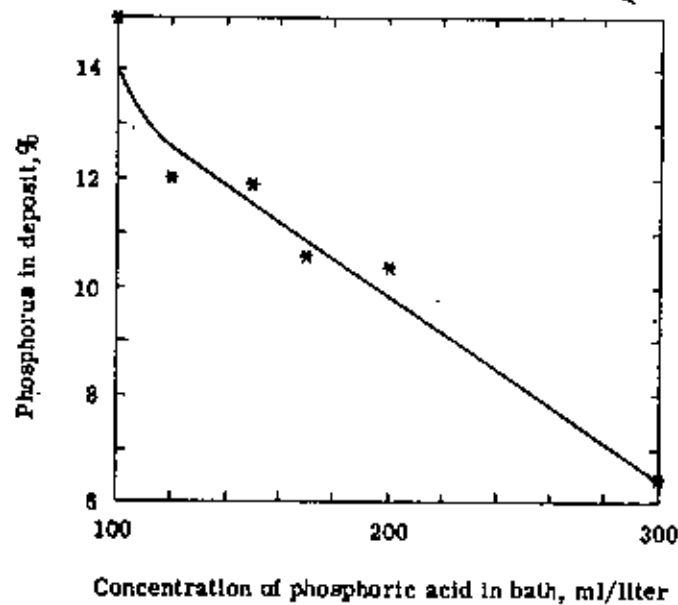


Fig. 2.4 Variation of the phosphorus content of electro-deposited nickel phosphorus alloys with the phosphoric acid content of the bath [18]. This curve represent nickel-phosphorus alloys deposited from bath F as given in Table 2.1. Current density: 40 amp/dm², Temperature: 90°C.

Careful control of the pH of the alloy plating baths was essential for obtaining sound deposits. If the pH of the bath became too high, basic material codeposited. The control of the pH of the bath requires fairly frequent measurement and adjustments, because the low cathode current efficiency tends to raise the pH, unless insoluble anodes are used. The acid is preferably added by continuous dripping, after the rate of consumption of acid by the bath has been determined. The direct measurement of the pH of highly acidic, concentrated solutions of metallic salts with a glass electrode some times yields incorrect results. The cause of the inaccuracy may be a dehydrating effect of the concentrated solution on the glass electrode.

2.4 VARIABLES OF BATH OPERATION

Deposition current density, bath temperature, bath agitation, types of anode and substrate are the main variable in the electrodeposition of nickel-phosphorus alloy. Information on these variables used by different researchers are shown in Table 2.2 . Wide variation in plating variables found in different works.

Current density used by different workers are found to vary widely. Higher current densities are found to be used by those employing a higher degree of agitation. Bath temperature for nickel phosphorus is mostly above 60°C.

Table 2.2 Summary of information of variables of bath operation used by different researcher for the electrodeposition of Ni-P alloy

Reference	Current density A/dm ²	Temp. °C	Bath Agitation	Substrate	Anode
Ratzkur et al. [16]	10-150	85	Constant pumping and filtering	Cu disk mounted on rotator	Platinum
Rajagopal et al [26]	15	60	uniform pumping	Mild steel	Nickel
Husheng et al [27]	1.0-1.5	60	—	Chilled cast iron	—
Brenner et al [4]	5-40	75-95	Air agitation	Steel	Nickel
Atanasiu et al. [18]	30	90	Air agitation	Steel	Platinum
Bredael et al [19] (For jet-cell)	2-150	60	Flow velocity, 4 m/s	Brass foil	Platinized titanium nozzle
Bredael et al [19] (For RDE)	2-150	65	Rotating speed 750 rpm	Circular brass discs	Platinized titanium grid
Toth Kadar et al [35]	0.70-10	70	Homogeneous agitation with laminar flow	Copper foils	Nickel plate

2.4.1 Effect of Current Density

Current density is the most important of the operating variables. The relations between the composition of the deposit and the current density in induced codeposition are similar to those of irregular codeposition. The effects of current density are not large and there is no consistent trend of the content of the reluctant metal in the deposit with current density. Typical curves are given in Fig. 2.5 showing the effect of current density on the compositions of alloys of three reluctant elements: Phosphorus, tungsten and molybdenum [13].

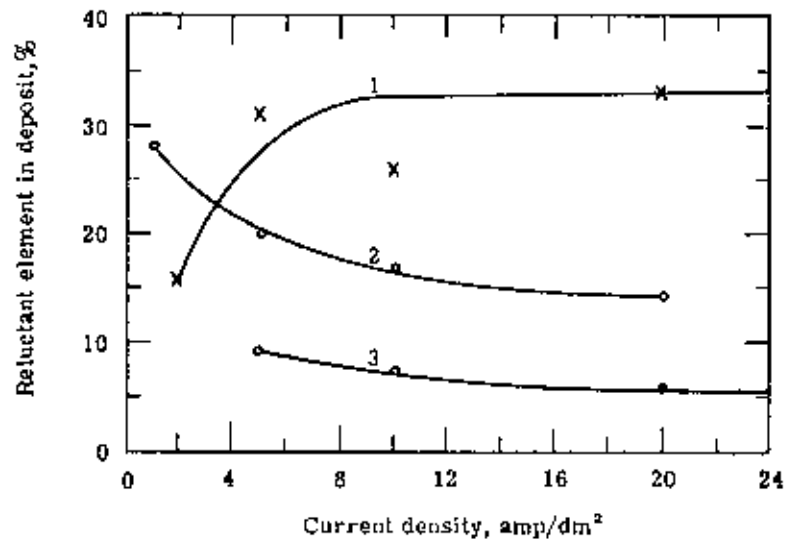


Fig. 2.5 Relation between alloy composition and current density in induced codeposition as illustrated by tungsten-nickel (curve 1), molybdenum-nickel (curve 2) and phosphorus-cobalt alloys (curve 3).

Curve 1 representing the deposition of nickel-tungsten alloys from an ammoniacal citrate bath shows an increase in tungsten content of the deposit with current density. Curve 2 representing the deposition of molybdenum nickel alloys from an ammoniacal citrate bath and curve 3 for the deposition of phosphorus-cobalt alloys from an acid bath, on the other hand shows a decrease in the content of the reluctant element with increase in current density [13].

The effect of current density on phosphorus content of deposit has been studied by different workers. Brenner [4] discussed the earlier works which are summarized in Fig.2.6. The phosphorus content of the deposits from baths high in phosphorus acid decreased as the current density was raised as shown in Fig. 2.6, but the content of phosphorus in the deposits of Ni-P alloys from the low phosphorus baths (data not shown in the figure) did not vary appreciably with current density [4, 18].

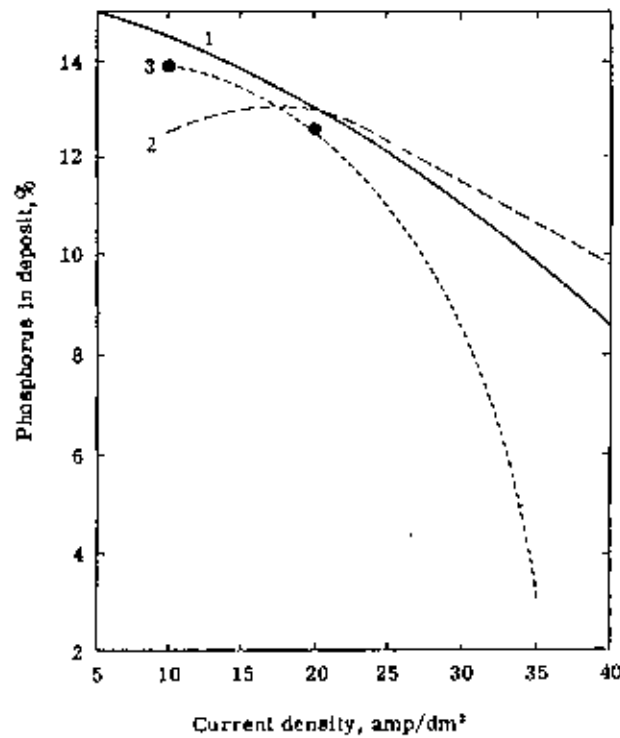


Fig. 2.6 Variation of the phosphorus content of electrodeposited nickel-phosphorus alloys with current density. Curve 1, nickel-phosphorus alloys deposited from the high-phosphorus bath E, as given in Table 2.1 for composition. Data of Brenner et al. [4]. Curve 2, nickel-phosphorus alloys deposited from the bath F, as given in Table 2.1, except concentration of H_3PO_3 was 25 g/l. Data of Atanasiu et al. [18]. Curve 3, nickel-phosphorus alloys deposited from the bath F, as given in Table 2.1, except concentration of H_3PO_3 was 10 g/l. Data of Atanasiu et al. [18].

More recent studies on the effect of deposition current density on the phosphorus content of the deposit was summarized by Bredael et al. [19] as presented in Fig.2.7. A general trend of a decreasing phosphorus content with increasing current density is evident. The large scatter in the results presented in Fig.2.7 is mainly due to the different bath composition used.

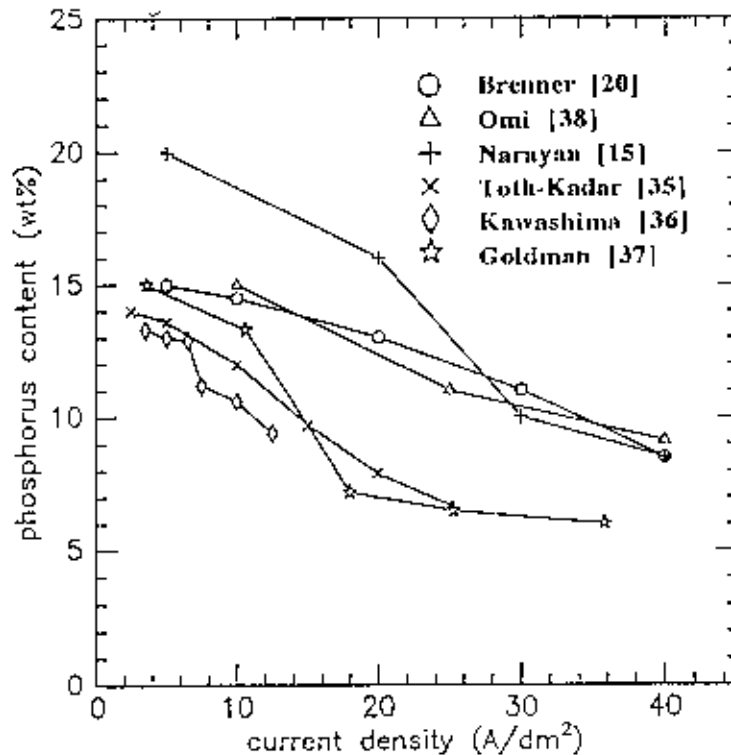


Fig. 2.7 Effect of current density on phosphorus content found by different investigators [15,20,35-38]

Bredael et al. [19] investigated the phosphorous content of the Ni-P coatings as a function of the current density in a jet-cell for baths (Table 2.1) containing varying amounts of phosphorous acid (H_3PO_3) as shown in fig. 2.8. There are two types of curves observed in this figure, one group (curves G, H, and I) indicating low phosphorus acid baths (baths G,H and I respectively , as given in Table 2.1) and other group (curves J, K, L) indicating high phosphorus acid baths (baths J,K and L respectively , as given in Table 2.1). The phosphorus content in the deposit is high at

lower current densities in the case of both types of baths. For baths with higher phosphorus acid, there is a transition current density below which the rate of increase in phosphorus content of the deposit with decreasing current density is low. Similarly, the rate of decrease of phosphorus content in deposit with an increase in current density is lower for deposition current densities above the transition value. The transition current density is found to be affected by phosphorus acid content in the bath. As the phosphorus acid content in the bath decreases, the transition shifts to lower values.

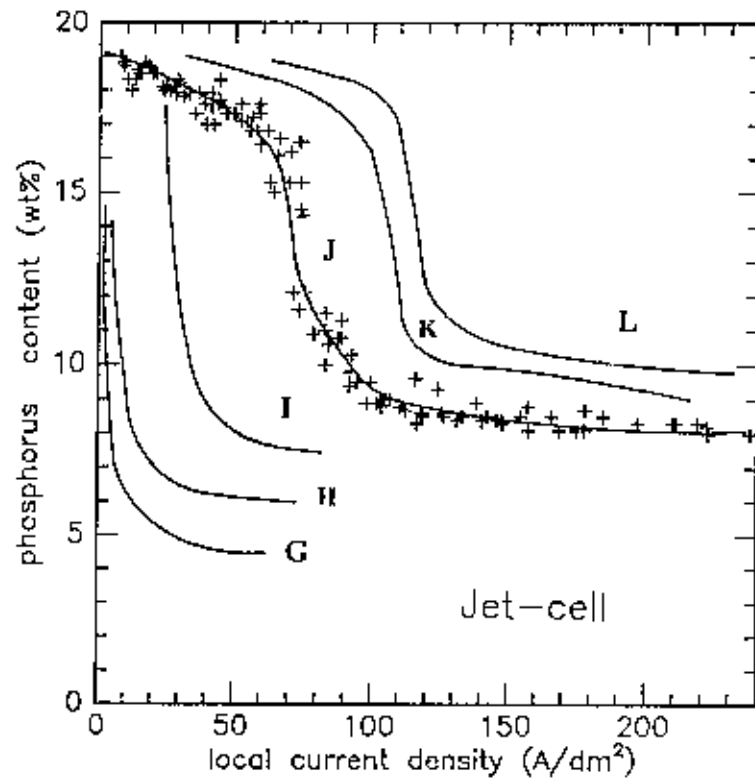


Fig. 2.8 Effect of current density in the jet-cell for different baths containing varying amounts of phosphorous acid. The curves represent data of Bredael et al.[19]. Curve G, nickel-phosphorous alloys deposited from bath G. Curve H, nickel-phosphorous alloys deposited from bath H. Curve I, nickel-phosphorous alloys deposited from bath I. Curve J, nickel-phosphorous alloys deposited from bath J. Curve K, nickel-phosphorous alloys deposited from bath K and Curve L, nickel-phosphorous alloys deposited from bath L. For composition of baths G, H, I, J, K and L, see Table 2.1.

The effect of current density on the cathode current efficiency of deposition of nickel-phosphorus alloys observed by Brenner [4] as shown in Fig. 2.9. The cathode current efficiency of deposition of the phosphorus alloys did not vary appreciably with current density, providing the current density was above the critical limit for deposition from the particular bath.

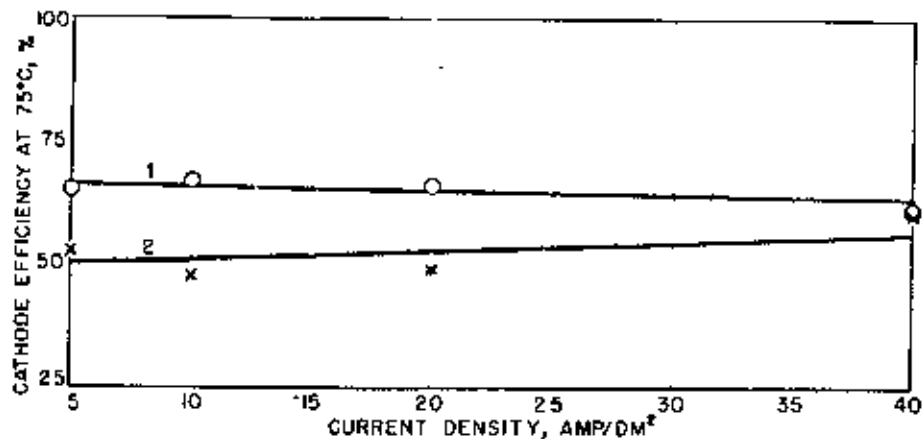


Fig. 2.9 Effect of current density on cathode current efficiency of deposition of nickel-phosphorus alloys. Baths operated at 75°C. Curve 1, nickel-phosphorus alloys deposited from low-phosphorus bath D and curve 2, nickel-phosphorus alloys deposited from high-phosphorus bath E, as given in Table 2.1 for composition. Data of Brenner et al. [4].

2.4.2 Effect of Operating Temperature

The effect of temperature on the composition of alloys in induced co-deposition is fairly consistent. An elevation of temperature of the bath usually causes a small increase in the content of the reluctant metal in the deposit [13]. Temperature was one of the most important variables governing the deposition of the Ni-P alloys. The deposits plated at room temperature were stressed and mechanically unsound and the cathode current efficiency of deposition was quite low [20]. Because of the unsatisfactory nature of the deposits obtained at room temperature, deposition was always carried out at elevated

temperatures. Brenner et al. considered 75°C as the optimum temperature, but Atanasiu et al. preferred 90°C. This latter temperature has some advantages. However, pitting was more serious at this temperature than at 75°C. Also at 90°C high current densities had to be used to obtain complete coverage of a specimen. The rapid evaporation of the bath at 90°C was another inconvenience [20]. The effect of temperature on the cathode current efficiency of alloy deposition is shown in Fig. 2.10.

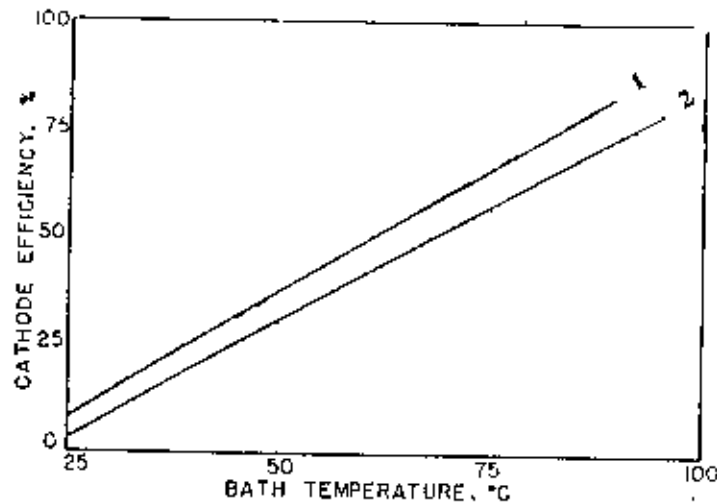


Fig. 2.10 Effect of bath temperature on the cathode current efficiency of deposition of phosphorus alloys. Data from Brenner et al. [4]. Curve 1, nickel-phosphorus alloys deposited from the low-phosphorus bath D of Table 2.1. Curve 2, nickel-phosphorus alloys deposited from the high-phosphorus bath E of Table 2.1.

2.4.3 Effect of Agitation

Uniform agitation over the cathode is most important in the deposition of Ni-P alloy. The deposition potential of Ni-P alloy and the phosphorus content of the deposit is directly affected by agitation.

Fig. 2.11 represents the importance of the bath agitation on the phosphorus content of the deposit, where, with exception of the bath agitation, nearly identical plating parameters were used in the two investigations. Lashmore and Weinroth [22] used a magnetic

stirring bar in their plating cell, while Ng et al.[23] deposited Ni-P coatings in a high speed deposition system with flow-rate up to 14 m/s. This higher agitation yields phosphorus-rich Ni-P coatings.

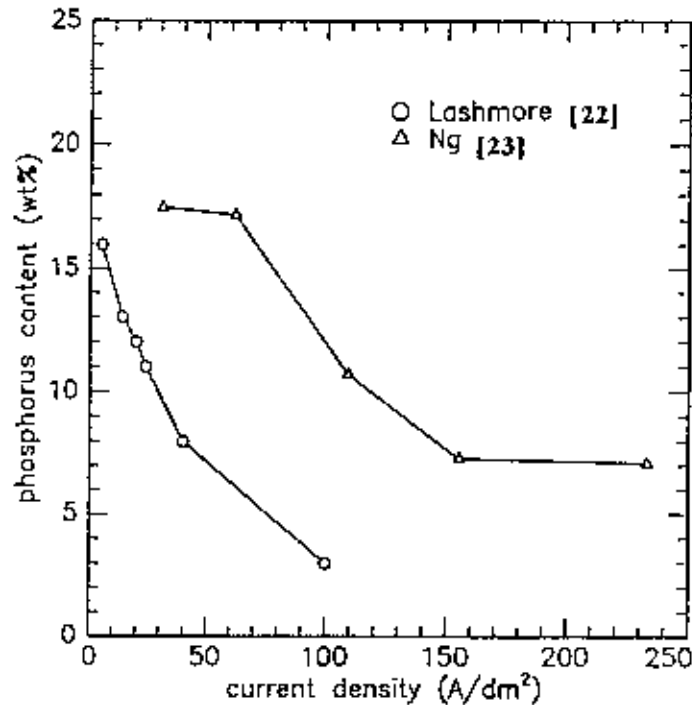


Fig. 2.11 Effect of bath agitation on phosphorus content of the deposit. Data of Lashmore et al.[22] and Ng et al.[23].

2.5 CURRENT DENSITY-POTENTIAL RELATIONS IN NICKEL-PHOSPHORUS ALLOY DEPOSITION

According to the hypothesis of the transfer of polarization, the upper theoretical limit for the content of phosphorus in the nickel alloy should be one equivalent of phosphorus to one of iron-group metal which corresponds to 25% phosphorus by weight. As already noted, the highest content of phosphorus obtained in an alloy was 15%. Atanasiu et al [18] obtained black deposits containing 33% phosphorus but they were not ductile.

The deposition potentials of the nickel-phosphorus alloy are more noble than that of nickel. This is shown in Fig. 2.12 by comparison of the current density-cathode potential curves for the deposition of nickel-phosphorus alloys, curves 1 and 2, with curve 3 for deposition of nickel individually. Similar observations were reported by Atanasiu et al. [24].

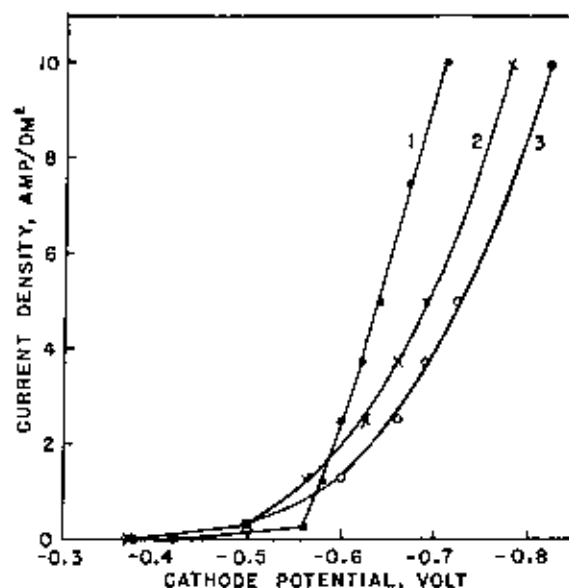


Fig. 2.12 Relation between current density and cathode potential in the deposition of nickel-phosphorus alloys. Temperature of deposition: 85°C. Data of Taylor [21]. Curve 1, nickel-phosphorus bath containing 35 ml/l of H_3PO_4 (85%) with addition of 115 ml/l of H_3PO_3 (70%). Curve 2, nickel-phosphorus bath containing 35 ml/l of H_3PO_4 (85%) with addition of 4 ml/l of H_3PO_3 (70%). Curve 3, nickel bath containing 35 ml/l of H_3PO_4 (85%).

The current density-cathode potential curve recorded by Bredael et al. [19] for the electrodeposition of Ni-P alloys in the jet-cell is shown in Fig. 2.13. Bredael et al. observed a transition potential at which the slope of the polarization curve changes. At potential more noble than the transition potential, higher phosphorus deposits were obtained. Potentials less noble than transition potential yielded deposits with low phosphorus.

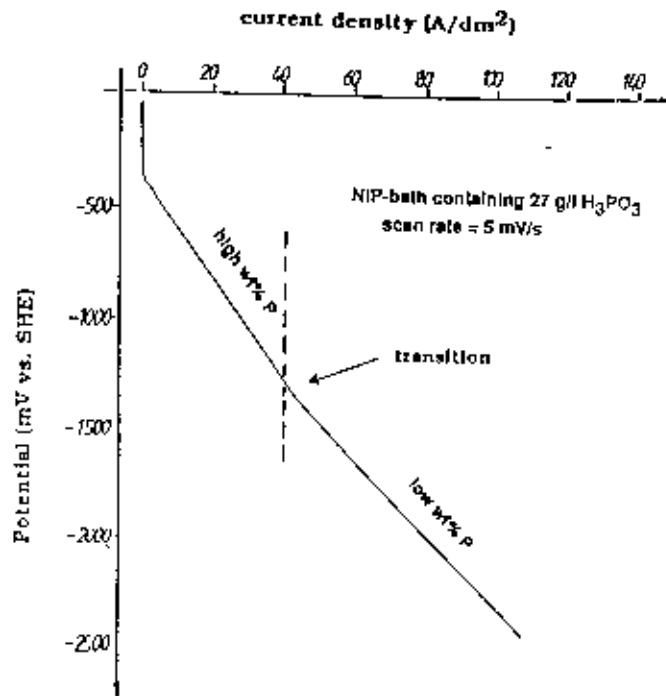


Fig. 2.13 Relation between current density and cathode potential in the deposition of nickel-phosphorus alloys. This curve was recorded in bath containing 27 g/l H_3PO_3 (bath I, as given in Table 2.1) at a temperature of $60^\circ C$ and a velocity of 4 m/s. Data of Bredael et al.[19].

2.6 STRUCTURE AND PROPERTIES OF ELECTRODEPOSITED NICKEL-PHOSPHORUS ALLOY

The properties of the electrodeposited NiP alloys are of special interest; partly because the alloys are the only ones that contain a non-metal and can be deposited in a sound condition; and partly because the properties themselves are unusual. The alloy can be electrodeposited bright without organic addition agents, it has high hardness, and an unusual structure. The deposits varied in appearance, depending on their content of phosphorus. Deposits containing 2% or less of phosphorus were smooth and fine-grained, but with a mat appearance very much like that of ordinary electrodeposited nickel. Deposits with a phosphorus content of about 5% were semi-bright and those with a phosphorus content above 10% were fully bright. These latter were true bright

deposits, because when formed on a dull surface they increased in brightness with increase in thickness. The reflectivity of buffed deposits which contained 2% of phosphorus was only slightly lower than that of the unalloyed iron-group metals. The as-deposited, bright deposits had a slightly dark or yellowish cast, as might be expected because of their larger content of phosphorus. Their specular reflectivity was only about 45 or 50% as compared with about 60% for nickel.

2.6.1 Structure of Deposits

2.6.1.1 Microscopic Examination

Microscopic examinations of electrodeposited phosphorus alloys were made by Brenner et al. [4], Atanasiu [18] and Goldstein [25]. The observations were similar. In studying the microstructure of the alloys Brenner et al. found some difficulty in finding etching reagents that did not produce pits [20]. The microstructure of nickel-phosphorus alloys containing 13% of phosphorus had many well-defined laminations and differed completely from the microstructure of unalloyed, electrodeposited nickel. The phosphorus alloys after heat-treatment, lost their characteristic lamination and developed a fine granular structure quite different from the large equiaxed grains obtained by heat-treating the pure metals [20].

2.6.1.2 X-ray Study

X-ray diffraction studies did not yield much information about the structure of the alloys. A specimen of the high-phosphorus nickel alloy yielded only one diffuse band which indicated that the material was amorphous and therefore, no information could be obtained about its structure. These amorphous alloys, being hard and brittle, might be considered as a metallic glass [20].

Bredael et al.[19] studied the structure of nickel-phosphorus alloys. X-ray diffraction was used to characterize the as-plated structure of Ni-P samples. It was observed that a transition from a structure with X-ray diffraction characteristics of amorphous materials to a crystalline structure takes place at 12% P. An important feature to be fulfilled, is that Ni-P coatings with a constant phosphorus content over the whole coating, have to be selected for the XRD experiments. Otherwise misleading results will be obtained. A broad XRD pattern as shown in Fig. 2.14(a) could result from an amorphous as well from a fine microcrystalline structure. The transformation occurring during heating an amorphous sample to a crystalline structure, can give some indirect information on the nature of the as-plated structure [32]. Chen and Spaepen [33] developed a calorimetric method in which an isothermal signal is used as a criterion to differentiate an amorphous structure from a crystalline one. This method has been applied by Bredael et al.[19] to the electrodeposited Ni-P samples and showed that above 12% P, real amorphous Ni-P coatings are obtained [19].

XRD measurements on compositionally homogeneous as-plated Ni-P deposits showed that above 12% P the as-plated coatings are amorphous, whereas below this threshold value, which is independent of the plating parameters crystalline Ni-P coatings are obtained [19]. The transition from the amorphous high phosphorus structure to the structure of crystalline one with a lower amount of phosphorus is possibly linked to a change in reaction mechanism of the Ni-P electrodeposition with increasing current density, as supported by electrochemical measurements [19]. Ni-P coatings with less than 12% P have a crystalline structure with a Ni (111) diffraction peak at 45 degrees 2θ and a Ni (222) diffraction peak at 98 degrees 2θ as shown in Fig. 2.14(b).

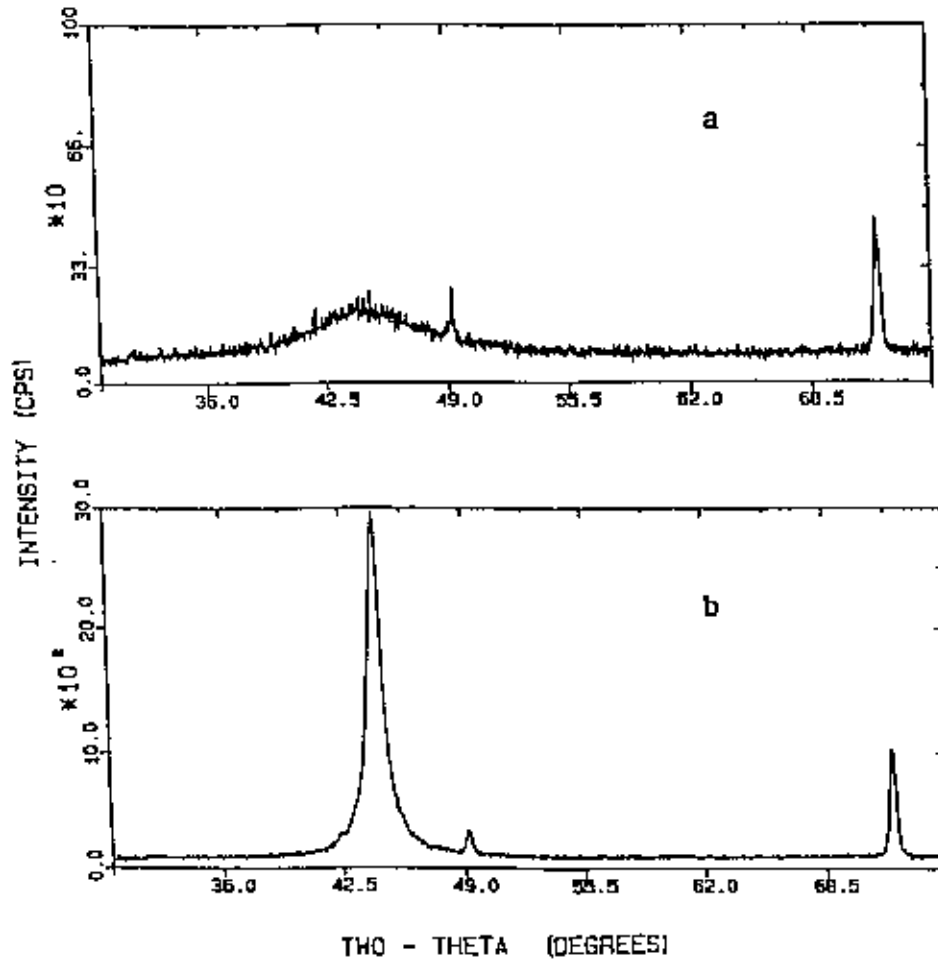


Fig. 2.14 (a) X-ray diffraction pattern of electrodeposited amorphous Ni-P alloys
(b) X-ray diffraction pattern of electro-deposited crystalline Ni-P alloys.

2.6.2 Physical and Mechanical Properties

2.6.2.1 Thickness

Thickness measurement on electrodeposited Ni-P coatings were carried out by Rajagopal et al. [26] with a pencil type magnetic thickness meter at 3 or 4 points on the specimen. Thickness of the Ni-P deposit were effected by the current density as shown in Table 2.3.

Table 2.3 Effect of current density on nickel-phosphorus alloy deposition [26]

Current density (A/dm^2)	Temperature ($^{\circ}C$)	Appearance of the deposit	Thickness of the deposite (μm)
50	60	Dull deposit	4-5-5
100	60	Non uniform deposit	10-12
150	60	Uniform and dull deposit	90-100

Duration of experiment : 60 min

pH : 3.5-4

Concentration of $NaH_2PO_4 \cdot H_2O$: 5 g/l

Thickness of deposit were also effected by the duration of the deposition [26] with Table 2.4.

Table 2.4 Effect of time on the Ni-P alloy deposition [26]

Duration of experiments (min)	Appearance of deposit	Thickness of the deposit (μm)
10	Very thin deposit	2
20	Thin deposit	4 - 7
30	Uniform, bright and adherent deposit	17 - 21

Current density : $150 A/dm^2$

Concentration of $NaH_2PO_4 \cdot H_2O$: 100g/l

pH : 2

Temperature : $60^{\circ}C$

Bredael et al.[19] electroplated Ni-P coatings on a rotating disc electrode(RDE) at average current densities up to 150 A/dm^2 in plating bath containing $40 \text{ g/l H}_3\text{PO}_3$ (bath J, as given in Table 2.1). The relationship between current density and thickness of the coatings as reported by Bredael et al. is shown in Fig. 2.15. With increasing average current density the layer thickness increases. For each average current density an increase in layer thickness is observed towards the edge of the cathodes. This increase is very pronounced for the coatings deposited at 40 and 60 A/dm^2 .

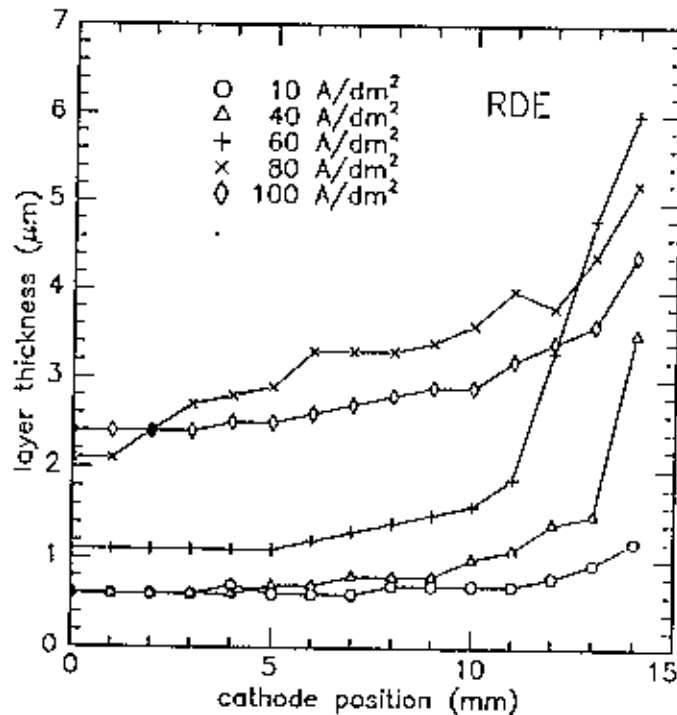


Fig. 2.15 Variation of layer thickness as a function of current density in the rotating disc electrode with respect of cathode position . The curves represent data of Bredael et al.[19]. For composition of bath , see Table 2.1.

2.6.2.2 Hardness

The vickers microhardness of the Ni-P amorphous coatings on substrates of steel 60Si 2Mn were measured by Husheng et al.[27] after heat treatment at different temperatures (Fig. 2.16.) . The microhardness changed little when the temperature was below 300°C . Above 300°C , it rose very quickly. The maximum value (1200 Hv) was reached at

430°C. Then the microhardness decreased and approached 770 Hv at 600°C. It can be seen from Fig. 2.16 that the microhardness of coatings was greater than 1000 Hv when the heat treatment temperature was between 380 and 480°C [27].

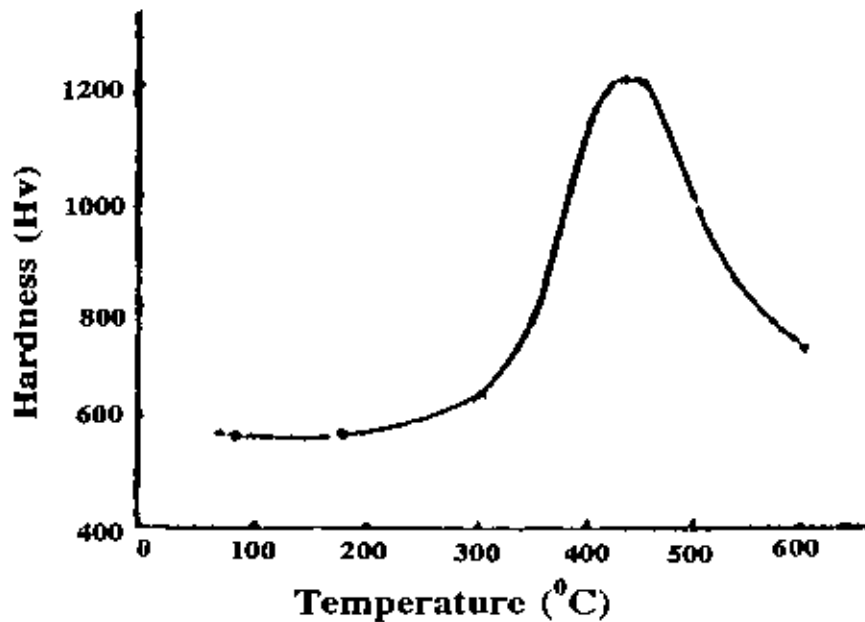


Fig. 2.16 Variation in microhardness of Ni-P coatings with heat-treatment temperature. Data of Husheng et al. [27].

The hardness of Ni-P coatings in the as-deposited and heat-treated condition were also measured by Brenner et al. [4] as shown in Fig. 2.17.

The phosphorus alloys of nickel increased in hardness on heat treatment. Brenner et al. [4] and Goldstein [25] made observations on the effect of heating. The maximum hardening was obtained at about 400°C. Deposits heated at 800°C were usually either of about the same hardness as initially or slightly softer. The high phosphorus-nickel alloy, curve 1, subjected to the heat treatment at 400°C became about as hard as electrodeposited chromium which usually has a hardness about 900 VHN. The phosphorus alloys were softened less than chromium due to exposure at 800°C.

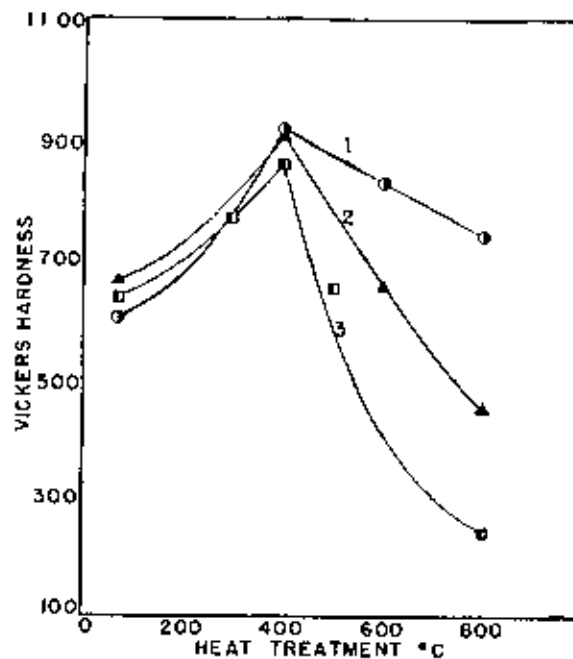


Fig. 2.17 Effect of 1 hour heat-treatment on the hardness of electrodeposited nickel-phosphorus alloys. Data of Brenner et al.[4]. Curve 1, nickel-phosphorus alloys containing 13-14% of phosphorus. Curve 2, nickel phosphorus alloys containing 6-7% of phosphorus. Curve 3, nickel phosphorus alloys containing 2-3% of phosphorus.

2.6.2.3 Strength and Ductility

Nickel alloys containing up to 2% of phosphorus are strong and slightly ductile. After heat treatment at the optimum hardening temperature of 400°C, the low-phosphorus alloys became more brittle, but after heat treatment at 800°C, they became more ductile than they were originally [4].

The higher the phosphorus content of the deposits, the weaker and more brittle they were. Heat treatment of the high-phosphorus alloys at 800°C caused them to become still more brittle and weaker than they were initially.

One interesting point yet to be settled is whether it is possible to find a temperature for heat treating the phosphorus alloys which will harden them and yet render them more ductile. In contrast, practically all thermally prepared alloys which are hardened by heat treatment also become less ductile. There is a basis for believing that electrodeposited alloys could become both harder and more ductile on heat treatment. If the low ductility of the electrodeposited alloys were partly due to internal stress, this could be relieved by heat treatment with an improvement in ductility [4].

2.6.3 Electrical and Magnetic Properties

The electrical resistivity of electrodeposited nickel is about 8 microhm-cm and that of electrodeposited cobalt is probably about the same. Fig.2.18 shows that the resistivity of the phosphorus alloys is considerably higher than that of unalloyed, electrodeposited nickel (curve 6) and that the resistivity increases with the phosphorus content of the deposits. Heat treatment of the alloys decreased the resistivity of the deposits, but the decrease leveled off for heat treatment above 600°C [4].

Brenner et al. [4] made measurements on the magnetic properties of the phosphorus alloys. Nickel alloys containing more than 8% of phosphorus were nonmagnetic.

Working with a sodium hypophosphite bath, Zhogina and Kznachei [28] deposited cobalt-nickel-phosphorus alloys for magnetic recording tapes. The coercive force of the alloy is shown in Fig. 2.19 as a function of the sodium hypophosphite concentration of the bath. The coercive force had a maximum of about 800 Oersteds. The phosphorus content of this deposit was about 3.3%.

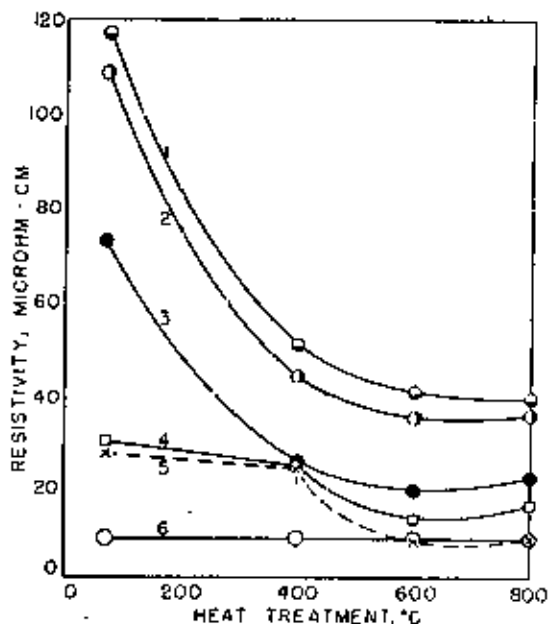


Fig. 2.18 Effect of 1 hour heat-treatment on the electrical resistivity of electrodeposited cobalt-phosphorus and nickel-phosphorus alloys. Data from Brenner et al. [4]. For composition of baths, see Table 2.1. Curve 1-3, represent nickel phosphorus alloys containing 13, 10 and 7% of P respectively. Curve 4, represent nickel-phosphorus alloy containing 2.2% of P. Curve 5, cobalt-phosphorus alloy containing 1.7% of P. Curve 6, unalloyed nickel deposited from bath contained no phosphorus acid.

2.6.4 Density

The density of phosphorus-nickel alloys decreased as the content of phosphorus in the deposit increased. The density of the deposits did not change appreciably as a result of heat treatment. Over the short range of compositions, the relation between density and content of phosphorus was nearly linear [20]. The densities of several thermally prepared nickel phosphide are given [29] as follows: Ni_3P : 7.8 g/cm^3 , Ni_7P_3 : 7.4 g/cm^3 , Ni_2P : 7.2 g/cm^3 ; $\text{NiP}_{0.82}$: 5.85 g/cm^3 . The best agreement with the experimental data was obtained with the Ni_3P .

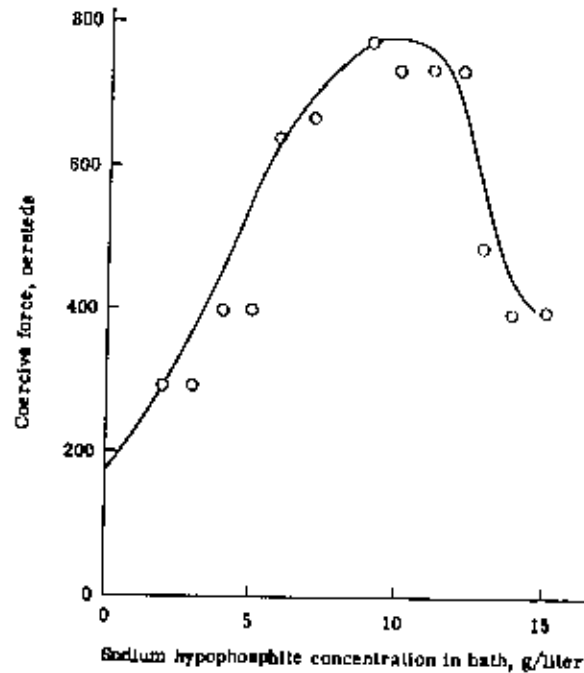


Fig. 2.19 Variation of Coercive force of electrodeposited cobalt-nickel-phosphorus alloys with sodium hypophosphite concentration of the bath. Data of Zhogina and Kaznachei [28].

2.6.5 Protective Value

A. Brenner [20] studied the corrosion resistance of Ni-P coating. He observed that bright coatings of nickel phosphorus alloys (containing 10-15% P), several microns in thickness, developed numerous rust spots after 2 days in the salt spray test, but deposits 25 μm or more in thickness did not develop rust spots after a week or two [20].

Clara Deminjer and Brenner [31] made a comparison of the protection against rusting afforded to steel by coatings of electrodeposited nickel phosphorus alloy in out door exposure tests. The coatings of the electrodeposited phosphorus alloy were 25 μm thick. The tests were made at Kure Beach, North Carolina and Washington, D.C. for 14 to 15 months. The electrodeposited high-P alloys containing about 9% of P were about

equivalent in their protective value to the best electroless nickel deposits and both afforded much more protection than unalloyed nickel coatings. The low-P alloys containing about 3% of P were more protective than nickel coatings but were inferior to the high-P coatings. The appearance of the high-phosphorus coatings was still very good after the exposure. Those exposed in Washington D.C. were still bright and by a slight amount of polishing could be restored readily to their original appearance.

Goldstein [25] also made observations on the protective value of nickel-phosphorus coatings. Those thicker than $25\ \mu\text{m}$ (1 mil) were stated to be free of pores, as-deposited and in out door exposure to afford steel better protection than nickel or chromium coatings.

2.6.6 Wear Resistance

Improved wear resistance has been observed in nickel-phosphorus alloy coatings in different studies. Husheng et al.[27] found that nickel-phosphorus coatings remarkably increase the sliding wear resistance of chilled cast iron [27]. They considered the use of nickel-phosphorus coatings on chilled cast iron tappets for improved performance.

Nickel-phosphorus alloy coatings offer good dry sliding wear resistance in the heat-treated state on 0-2 steel [30]. An investigation of dry sliding wear of electrodeposited nickel-phosphorus coatings on 0-2 tool steel against 52100 steel has been carried out by Ruff et al.[30]. Wear test on the uncoated 0-2 tool steel material has also been carried out for comparison. From this study of dry sliding wear characteristics of Ni-P alloy coatings on 0-2 steel, it has been seen (Table 2.5) that after heat treatment (at 400°C for 30 min.) all the nickel-alloy coatings developed a significantly greater wear resistance than uncoated 0-2 tool steel.

Table 2.5 Comparison wear rate between 0-2 tool steel with Ni-P alloy coatings and without coatings [30]

Coating <u>Designation</u>	Substrate <u>Designation</u>	Wear rate <u>$10^{-4} \text{ mm}^3/\text{m}$</u>
Uncoated	0-2 steel	1.1
Ni-5P, DC, HT	0-2 steel	0.17
Ni-12P, PP, HT	0-2 steel	0.12
Ni-12P, DC, HT	0-2 steel	0.31

DC= direct current; HT = heat treated; PP=pulse plated

CHAPTER: THREE

3. EXPERIMENTAL

3.1 SUBSTRATE PREPARATION AND ELECTRODEPOSITION

3.1.1. Substrate Preparation

In the investigation, copper sheet and cylindrical brass rod were employed as substrate and platinum sheets as anodes. Deposit made on copper sheets were used for chemical analysis, X-ray diffraction, thickness and hardness measurements while those on brass rod were used for wear studies.

The substrate pretreatment sequence used in this study is : 1) polishing 2) rinsing 3) alkaline degreasing 4) rinsing 5) acid dipping 6) rinsing (Fig.3.1).

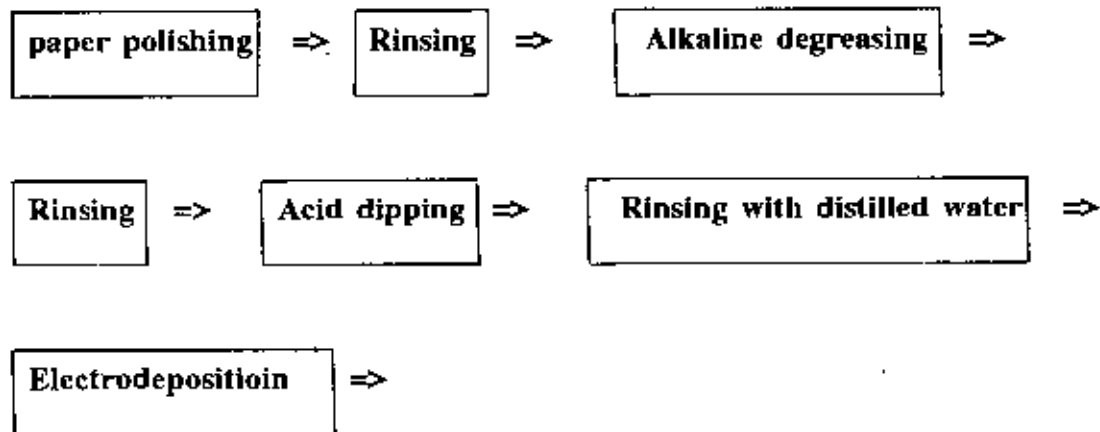


Fig. 3.1 Sequence of substrate pretreatment.

Polishing: The substrates were first polished with emery papers (sequence of paper grade: 3, 2, 1, 0, 2/0, 3/0, 4/0) to a fine finish .

Alkaline decreasing: The specimens were then cleaned in alkaline solution containing 35 g/l sodium carbonate (Na_2CO_3) and 25 g/l sodium hydroxide (NaOH) at 55°C for one minute .

Acid dipping: Traces of alkali on the surface were subsequently neutralized by dipping the specimens for 30 seconds in 10% sulfuric acid and was thoroughly washed with running water and then with distilled water.

3.1.2 Electrodeposition Set-Up

The electrodeposition set-up consists of a glass beaker, a d.c power supply, a magnetic stirrer, a thermometer, and a perspex electrode holder. The beaker containing the electroplating solution and a magnetic stirrer bar was placed upon a magnetic hot plate so as to heat the solution to a desired temperature and agitate it automatically. Cathode was connected to the negative terminal of the d.c. power supply via a multimeter and anodes were connected to the positive terminal.

For electrodeposition on copper sheets, two anodes were used on both sides of the cathode to achieve uniform deposition on both faces . Three equally spaced anodes placed around the substrate were used to deposit on cylindrical brass specimens. A thermometer was placed in the beaker and was used for measuring the temperature of the bath solution. The cross-section of the electrodeposition cell arrangement is shown in Fig 3 2.

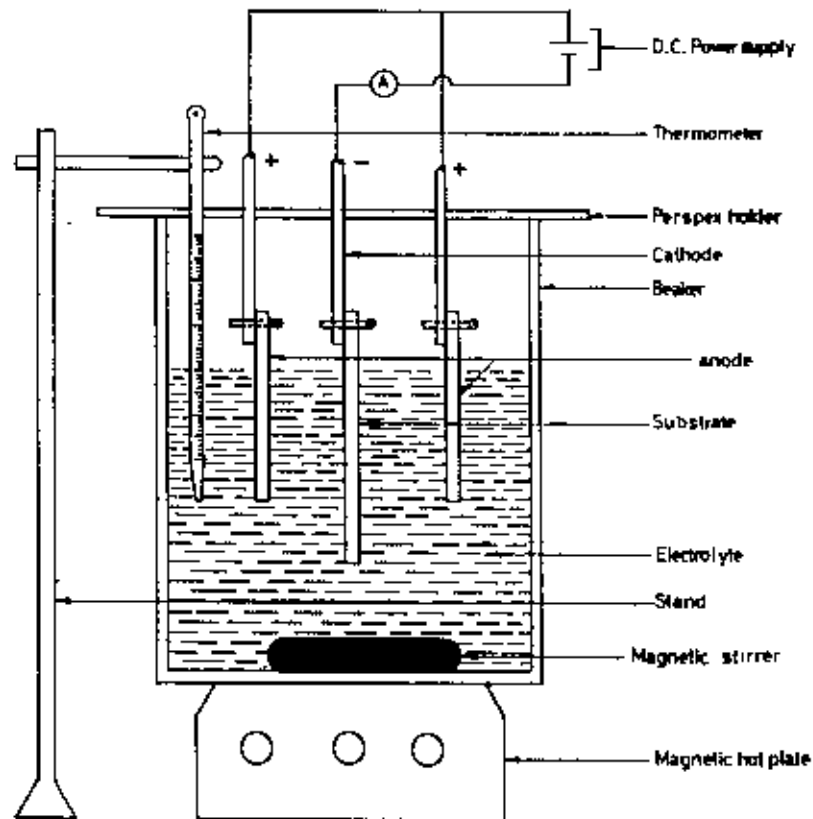


Fig. 3.2 Schematic diagram of a electrodeposition unit.

3.1.3 Electroplating Operation

After the preparation as described in section 3.1.1, the specimen was placed in a 1000 ml. capacity beaker which was filled approximately two-thirds with bath solution. The temperature of the bath solution was maintained at $60 \pm 3^\circ\text{C}$ using a thermostat and measured with a thermometer. The substrate was then connected to the negative terminal of a power supply and the platinum plates used as the anodes to the positive terminal. Deposition was carried out at constant current density. Current densities used in this study were 40, 60, 80, 100 and 200 mA/cm^2 . At the end of electrodeposition for a predetermined time period which varied from 1 to 7 hours, the power supply was

switched off and the specimen was taken out. After deposition, the specimen was thoroughly swilled in water to remove surplus electrolyte. The specimen was then dried and stored in a desiccator for further investigation. Composition of the plating baths and operating conditions are listed in Table 3.1 and Table-3.2 respectively.

Table-3.1 Composition of the Plating Baths

Baths Desig.	NiSO ₄ .6H ₂ O (g/l)	NiCl ₂ .6H ₂ O (g/l)	NaH ₂ PO ₂ .H ₂ O (g/l)	H ₃ PO ₄ (g/l)
I	150	45	75	50
II	150	45	100	50
III	150	45	125	50

Table-3.2. Operating Conditions of Ni-P Deposition

Parameters	Details
Current density (mA/cm ²)	60-200
Operating temperature (°C)	60 ±3°C
Operating time (Hours)	1 - 7
pH	1.63 at 60°C *
Degree of agitation	Mild

* For bath II (see Table 3.1)

For wear tests , deposits with a constant thickness of 20 μm were made at current densities of 60 and 100 mA/cm² . The deposition time for each current density was found out from a thickness versus deposition time curve (Fig.4.5) which was first established before depositing wear test specimens .

3.2 CHARACTERIZATION OF NICKEL-PHOSPHORUS COATINGS

3.2.1. Microhardness Measurement

All the coatings used for microhardness measurements were deposited on copper sheets. The vickers microhardness of the Ni-P coatings was measured with a Shimadzu microhardness tester. The load for measuring the hardness was 50 gm. This load was applied for 5 seconds . Microhardness measurements were done for deposits obtained at current densities of 60, and 100 mA/cm² from all the baths. By measuring the diagonal length of the indentations, VHN at the corresponding point was obtained from the calibration chart.

3.2.2. X-ray Diffraction

X-ray diffraction was used to characterize the as-plated structure of Ni-P samples. For this purpose, a JEOL X-ray diffractometer was used with copper k_α radiation. Details of the operating conditions of X-ray diffractometer are shown in Table-3.3.

Table 3.3 Operating Conditions for X-ray Diffraction

Radiation	:	Copper K _α
Voltage	:	30 kV
Current	:	15 mA
Scanning speed	:	1°/min
Chart speed	:	10 mm/min
Range	:	30°-100°

3.2.3 Chemical Analysis

The deposit was chemically analyzed for phosphorus and nickel content was found out by subtraction. To find out the phosphorus content, the deposit was removed from the substrate and 0.2 gm of the deposit was taken. The sample was dissolved in 20 ml. of 1:1 nitric acid. It was then diluted to 250 ml. 15 ml of this solution was taken and transferred to a 500 ml beaker. 45 ml. of HNO_3 was added and the solution oxidized with KMnO_4 after boiling off nitrous fumes. A brown precipitate was formed after 3-5 minutes of continuous boiling. Reduction was carried out with NaNO_2 and boiled for a few minutes to expel nitrous fumes. Temperature of the solution was adjusted at 45°C and 60 ml. Cold ammonium-nitro-molybdate was added. The solution was then shaken out for ten minutes and settled for 20 minutes at room temperature.

The precipitate and pad was transferred to the flask after filtering and washing. Sufficient amount standard NaOH solution was added then from a burette to dissolve the yellow precipitate. A few drops of indicator solution (phenolphthelin reagent) was added and titrated with standard 0.1N HNO_3 until the pink colour disappears. Assuming the standard solution are of equal strength. Phosphorus content was carried out from the following:

$$\% \text{ of P} = (\text{ml. of NaOH} - \text{ml. of HNO}_3) \times 1.67 \text{ on } 0.2 \text{ gm. sample}$$

3.3 WEAR TESTS AND EVALUATION

Wear tests were carried out in a pin-on-disc type apparatus (Fig. 3.3) under dry sliding conditions in the ambient air at room temperature. $20 \mu\text{m}$ thick Ni-P coating deposited on brass pin of 8 mm diameter and 6.5 mm length were used in this study. Brass pins without coatings were also tested for comparison.

Grey cast iron discs of 80 mm diameter and about 10 mm thickness were used as the counter body. During the tests, the plated cylindrical pin was pressed against the rotating disc under a constant load for a pre-specified time period. The disc speed was 500 rpm which gave a linear speed of 416 m/s at wear track.

For each experiment a new pin and a new disc were used. Before the tests, both the pin and disc were degreased, cleaned thoroughly in water and dried immediately in acetone. All tests were carried out in ambient air at room temperature. 180, 250 and 480 gm loads were used during the tests. Testing periods were 5, 10 and 15 minutes.

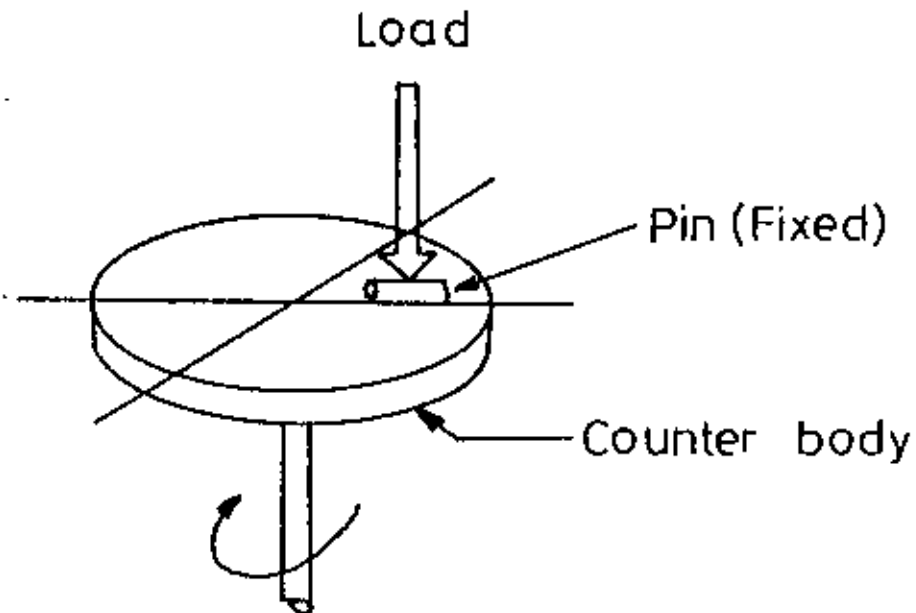


Fig. 3.3 Schematic diagram of wear test apparatus.

After testing, the worn surface of the pin was examined by optical microscopy and the width of the wear track was measured. At least three tests were carried out for each set of conditions and the average width track on pin was taken as a measure of the coating wear.

CHAPTER: FOUR

4. RESULTS AND DISCUSSION

4.1 COMPOSITION AND STRUCTURE

The effect of deposition current density on the phosphorus content of the Ni-P deposits is shown in Fig.4.1. It is seen from the figure that an increase in current density from 60 to 200 mA/cm² does not cause any significant variation in phosphorus content.

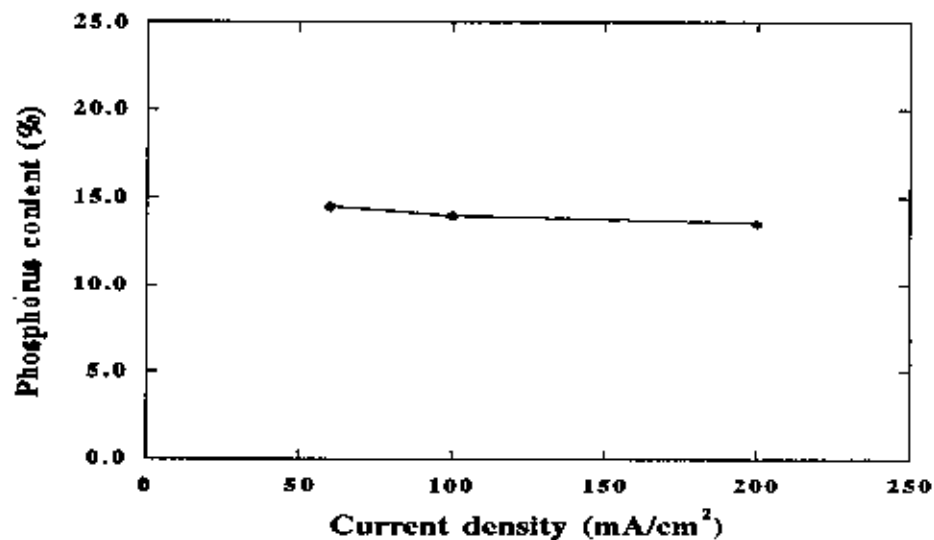


Fig.4.1 Effect of deposition current density on the phosphorus content of Ni-P deposits obtained at 60°C from bath containing 100 g/l sodium hypophosphite(bath II,Table 3.1).

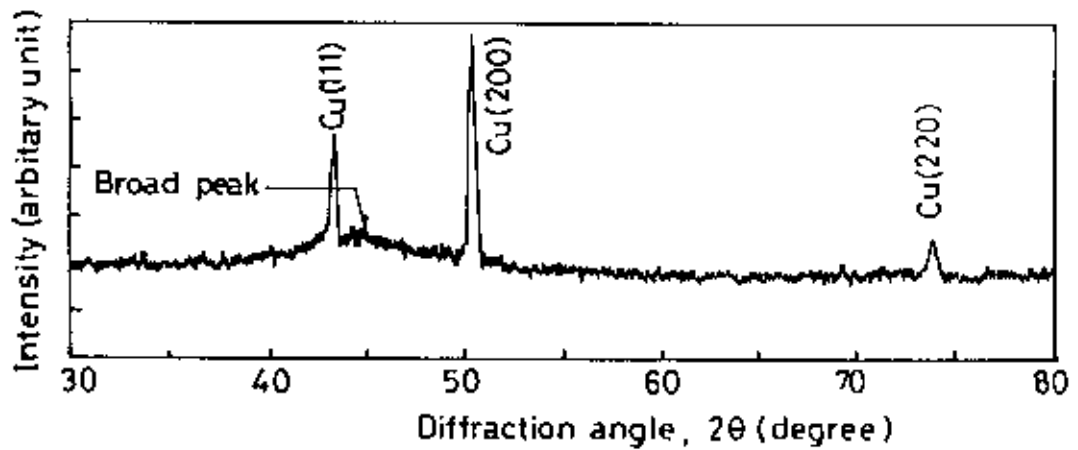
All the deposits obtained at 60, 100 and 200 mA/cm² contain about 14 wt.% phosphorus. The relationship between deposition current density and phosphorus content of the deposits obtained from baths containing phosphorus acid is well described in the literature. However the dependence of phosphorus content on current density in hypophosphite based bath as was used in the present work is not available.

Different studies on the relation between current density and phosphorus content in deposits from phosphorus acid-based baths have been summarized by Bredael et al.[19]. A general trend of a decreasing phosphorous content with increasing current density was observed in these investigations (Fig. 2.7). Similar observation was also made by Brenner [4] from the compilation of results of earlier studies. The range of current densities used in those earlier works in phosphorus acid based baths was very wide (20 to 400 mA/cm²) (Fig.2.7). In comparison, the currently studied current density range is only 60-200 mA/cm². This narrow range may hide the general trend that occurs over a wide current density range. It is therefore not clear whether the relative insensitivity of phosphorus content of the deposit to current density found in the present study is due to narrow current density range used or to the nature of the bath (i.e. hypophosphite based bath) employed. Further study is necessary to clarify this point.

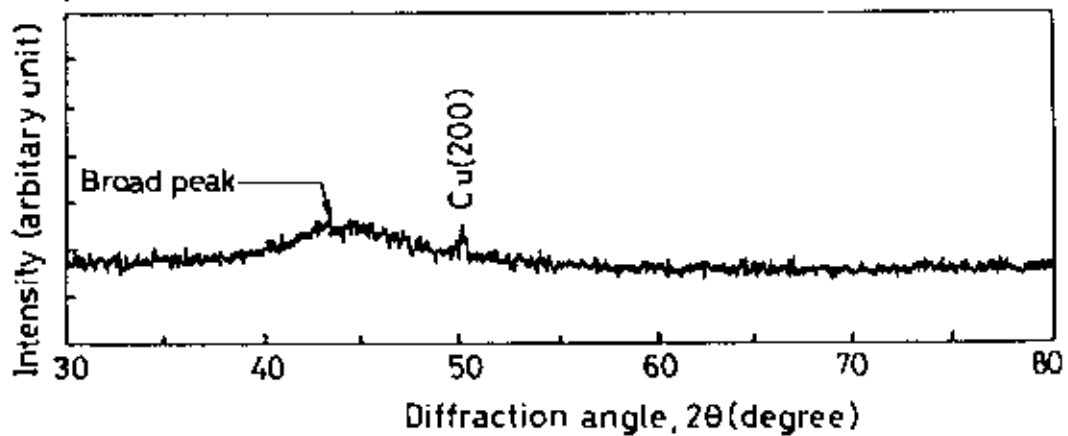
Amount of hypophosphite present in the bath was found to have a profound effect on the nature of the Ni-P deposits. It was found that there is an optimum hypophosphite concentration which yielded uniform, bright deposits. In the present study, this optimum concentration of sodium hypophosphite was found to be 100 g/l. This result confirms similar observation made by Rajagopal et al.[26] in an earlier study.

Ni-P alloy coatings deposited on copper substrate at different current densities were investigated by X-ray diffraction. X-ray diffraction pattern was also recorded on pure copper substrate. Fig. 4.2 shows the diffraction patterns of the above Ni-P alloy coatings and pure copper substrate. Patterns from all the coatings show a broad diffraction peak at 2θ value between 40-50°. The pattern from deposit obtained at 60 mA/cm² shows, in addition to the broad peaks, some extra sharp peaks. Comparing with the diffraction pattern of copper substrate (Fig.4.2d), it is clear that these extra peaks in Fig.4.2a actually belong to the substrate. Presence of the peaks of copper substrate in the diffraction pattern of Ni-P deposit obtained at 60 mA/cm² indicates lower thickness of the deposit. Thus all the deposits obtained at 60, 100, and 200 mA/cm² have a broad

diffraction peak in their diffraction pattern. This suggests an amorphous as-plated structure in all these deposits. It may be mentioned that all these deposits have similar phosphorus content, around 14 wt% .



(a)



(b)

Fig. 4.2 X-ray diffraction pattern of (a) Ni-P coating deposited at current density 60 mA/cm^2 (b) Ni-P coating at current density 100 mA/cm^2 ($\text{NaH}_2\text{PO}_2 \cdot \text{H}_2\text{O}$: 100 g/l, deposition time : 2 hours).

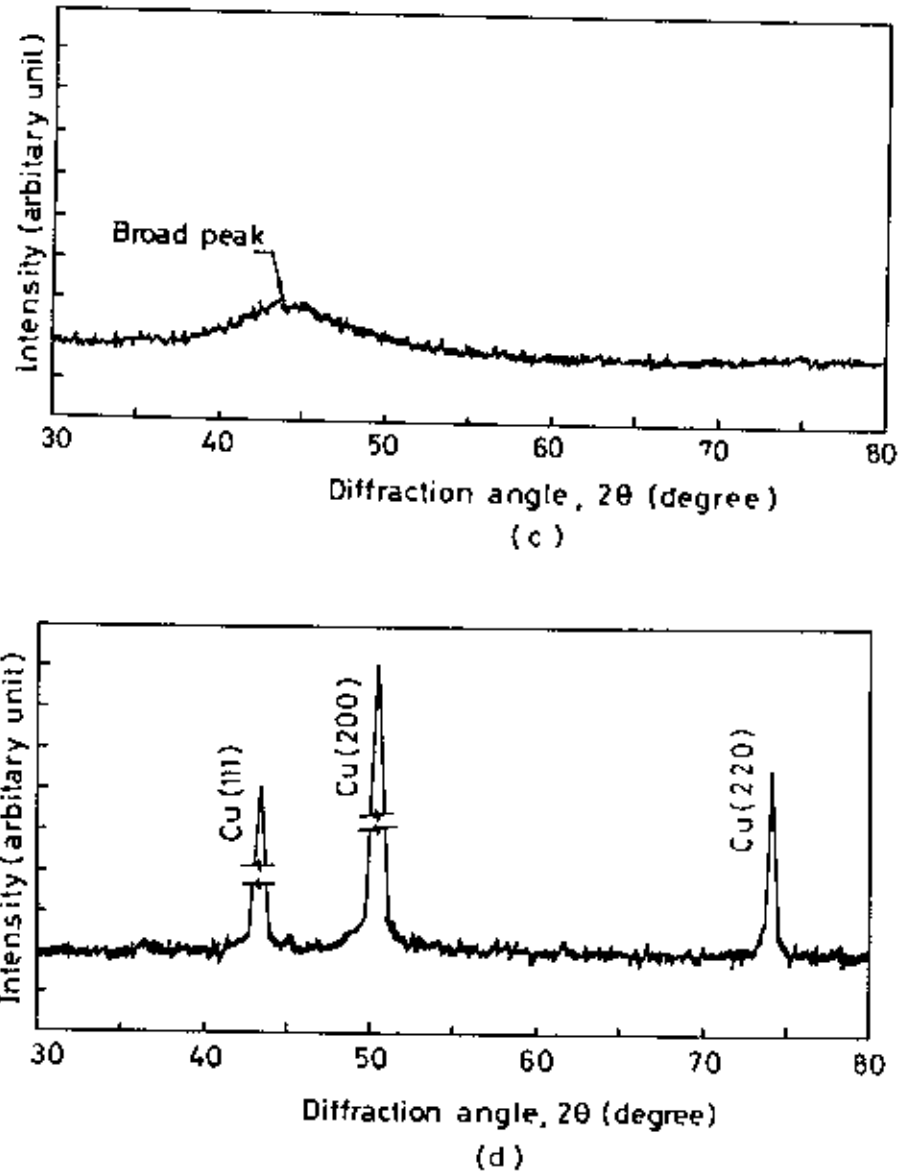


Fig. 4.2 (continued) (c) Ni-P deposited at 200 mA/cm^2 and (d) Pure copper substrate.

It is generally believed that Ni-P coatings becomes amorphous when the phosphorus content of the deposit exceeds a certain minimum value. In literature there is, however, no agreement on the exact phosphorous content where an amorphous structure is obtained in as-plated Ni-P alloys. The minimum phosphorus content for amorphous structure as found in different studies is compiled in Table 4.1.

It is expected in the present study where phosphorus content is 14%, that the structure of Ni-P deposits would be amorphous.

Table 4.1 Minimum Phosphorus Content for Amorphous Structure

References	Minimum phosphorus content for amorphous structure (wt%)
Rajagopal et al. [26]	12
Husheng et al. [27]	8
Bredael et al. [19]	12
Goldenstein et al.[41]	7-10
Graham et al. [34]	12

However, a broad XRD pattern, does not always guarantee a real amorphous structure. It could result from an amorphous as well from a fine microcrystalline structure. The transformation occurring by heating an amorphous sample to a crystalline structure, can give some indirect information on the nature of the as-plated structure [32]. Chen and Spaepen [33] developed a calorimetric method in which an isothermal signal is used as a criterion to differentiate an amorphous structure from a crystalline one. This method was applied by Bredael et al.[19] to their electrodeposited Ni-P samples and found that above 12% P real amorphous Ni-P coatings are obtained. This latter criteria suggests that Ni-P deposits containing about 14 wt% P obtained at 60-200 mA/cm² in the present study are real amorphous.

All the nickel-phosphorus deposits described above (Fig.4.2) were obtained from bath containing 100 g/l sodium hypophosphite. When the hypophosphite concentration in the bath was reduced to 5 g/l, the resulting structure of the deposit became crystalline (Fig.4.3).

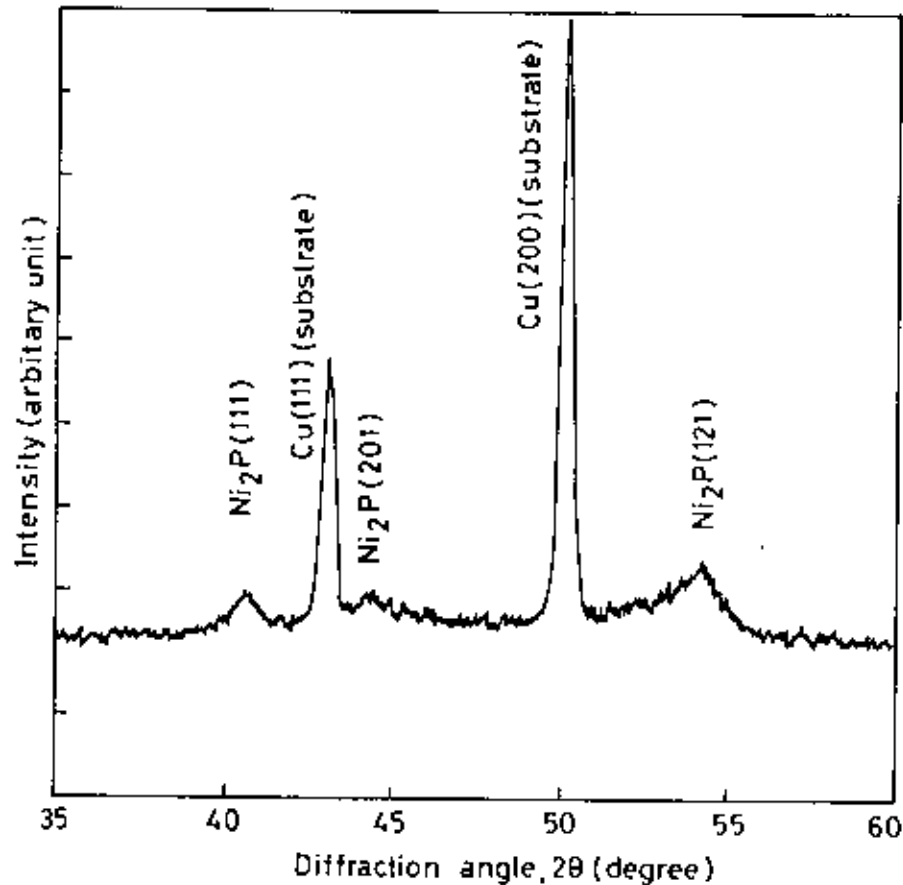


Fig.4.3 X-ray diffraction pattern of crystalline Ni-P alloy coating deposited at current density 400 mA/cm^2 ($\text{NaH}_2\text{PO}_2 \cdot \text{H}_2\text{O}$: 5 g/l, deposition time: 4 hours).

This deposit is seen to contain mainly Ni_2P compound. Peaks of copper substrate are also visible in the diffraction pattern. Since this deposit was dark and non-uniform, it was not used in any further study.

4.2 THICKNESS AND MICROHARDNESS

Variations in the thickness of Ni-P alloy coatings were observed in relation to the amount of sodium hypophosphite ($\text{NaH}_2\text{PO}_2 \cdot \text{H}_2\text{O}$) in deposition bath, current density and electrodeposition time. Fig. 4.4 shows the effect of current density and amount of $\text{NaH}_2\text{PO}_2 \cdot \text{H}_2\text{O}$ in the bath on coating thickness. It is observed that an increase in the amount of $\text{NaH}_2\text{PO}_2 \cdot \text{H}_2\text{O}$ in plating solution causes a decrease in coating thickness. On

the other hand, increasing the current density causes an increase in deposit thickness. It is seen in Fig.4.4 that the decrease in thickness with an increase in hypophosphite concentration is very pronounced at deposition current density of 80 mA/cm^2 . It is thought that an increase in the amount of hypophosphite favours hydrogen evolution at the cathode thereby decreasing current efficiency. This results in a lower thickness at higher hypophosphite concentration in the bath. It is evident from the Fig. 4.4 that the coating thickness is maximum when $75 \text{ g/l NaH}_2\text{PO}_2\text{H}_2\text{O}$ present in the plating bath. However the appearance and character of the deposit was not the best at the hypophosphite concentration of 75 g/l . In fact, deposit with best appearance and adherence was obtained when hypophosphite was present at a concentration of 100 g/l . At this concentration the deposit was bright and smooth. Similar observation was also made by Rajagopal et al.[26].

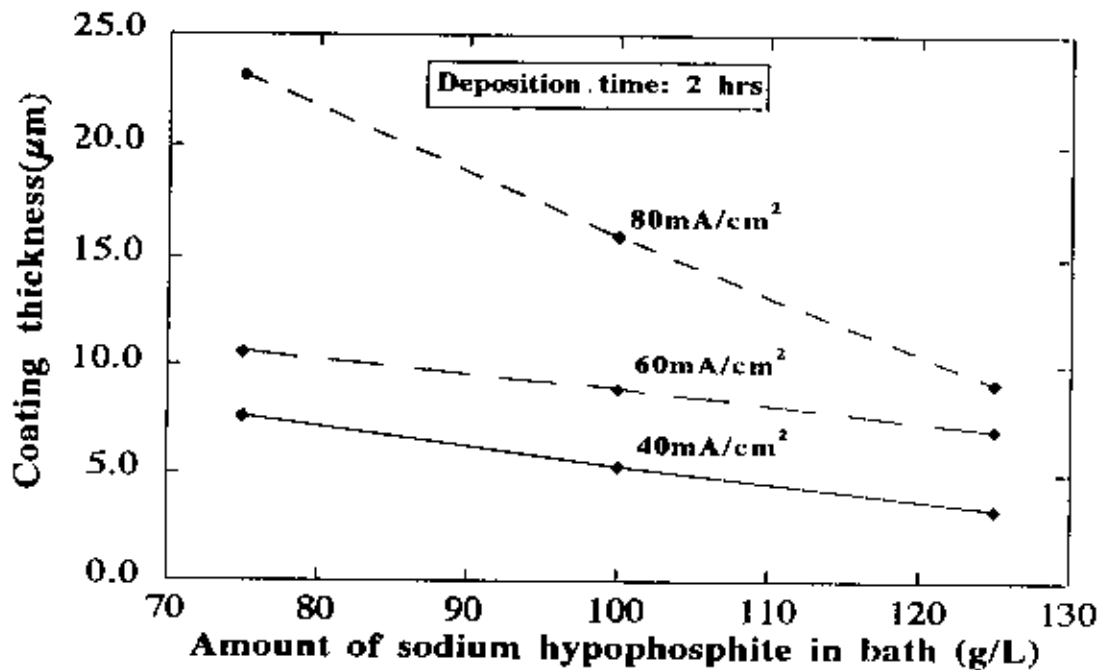


Fig. 4.4 Effect of amount of sodium hypophosphite in the plating bath on coating thickness (Deposition time: 2 hours).

The variation of coating thickness with deposition time is plotted in Fig.4.5. All the coatings were deposited from baths containing 100 g/l hypophosphite. Coating thickness data for three different current densities are plotted. It is seen that thickness of the deposit increases almost linearly with deposition time. Increasing deposition current density also causes an increase in coating thickness. This is in general agreement with Faraday's law of electrolysis. It may be mentioned that Fig.4.5 was used to find out time required to deposit 20 μm thick coatings at 100 mA/cm^2 and 60 mA/cm^2 for using in wear tests. The time periods required to deposit 20 μm thick Ni-P coating at 100 and 60 mA/cm^2 are 1 and 4 respectively. It is to be noted here that these time periods are much longer than the corresponding theoretical time periods. This is due to lower current efficiency caused by high hydrogen evolution in Ni-P plating baths [20].

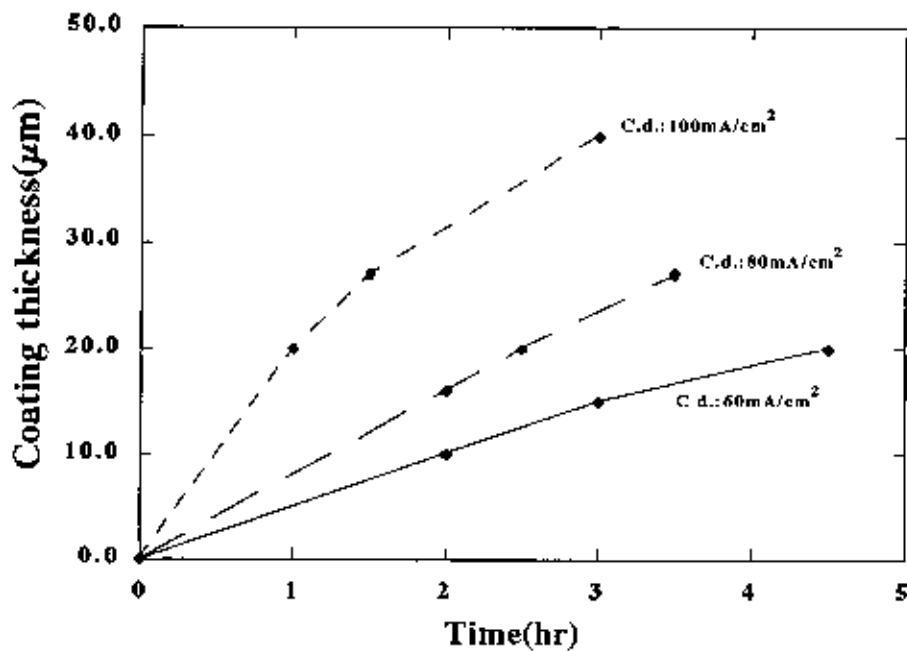


Fig.4.5 Effect of electrodeposition time and current density on coating thickness ($\text{NaH}_2\text{PO}_2 \cdot \text{H}_2\text{O}$: 100 g/l)

The microhardness of Ni-P coatings was found to vary with the amount of sodium hypophosphite in deposition bath. The effect of the amount of hypophosphite in deposition bath on microhardness is shown in Fig. 4.6. It is seen that within the range of

the amount of hypophosphite (75-100 g/l) studied, increasing the amount of hypophosphite at first causes an increase in the microhardness. The microhardness then decreases showing a peak value at a hypophosphite concentration of 100 g/l. Similar results have been reported in literature [26]. Rajagopal [26] found that harder deposit were obtained from bath containing 100 g/l $\text{NaH}_2\text{PO}_2 \cdot \text{H}_2\text{O}$.

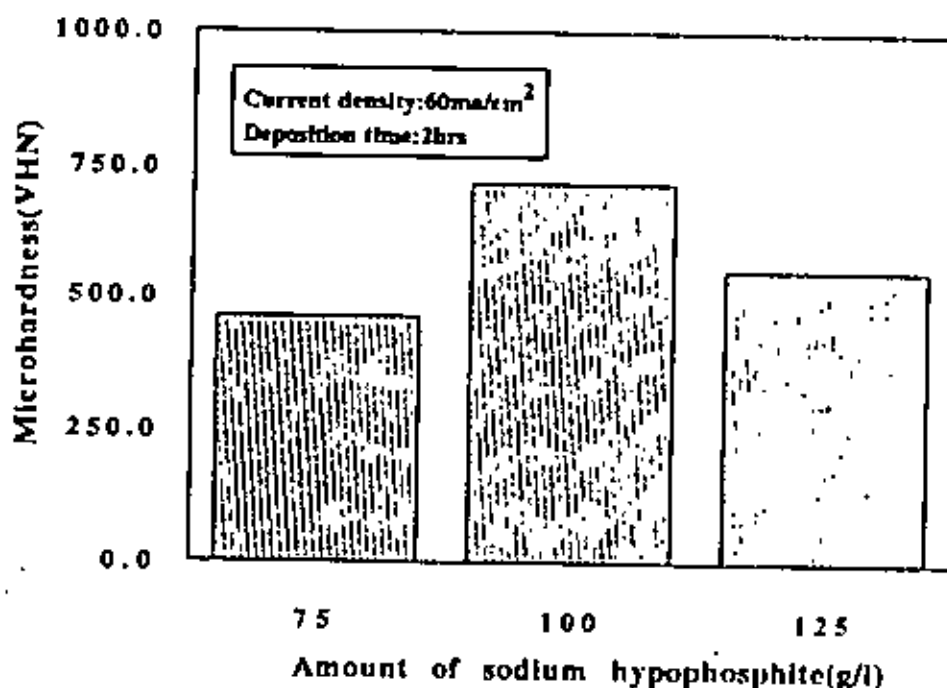


Fig. 4.6 Variation in microhardness of Ni-P coatings with the amount of sodium hypophosphite in bath solution (current density: 60 mA/cm², electrodeposition time: 2 hours).

The hardness value of as-plated deposits obtained at 60 and 100 mA/cm² from 100 g/l hypophosphite containing bath are given in Table 4.2 along with the data reported in literature. It is seen that hardness of the deposits obtained in the present study is quite high as compared with those reported in the literature.

Table 4.2 Hardness of As-Deposited Nickel-Phosphorus Coating

References	Hardness of as- deposited Ni-P coating (VHN)	Phosphorus content present (%)
Rajagopal et al. [26]	366	12
Brenner et al. [20]	600	13
Present investigation:	701*	14.28
	665**	14.13

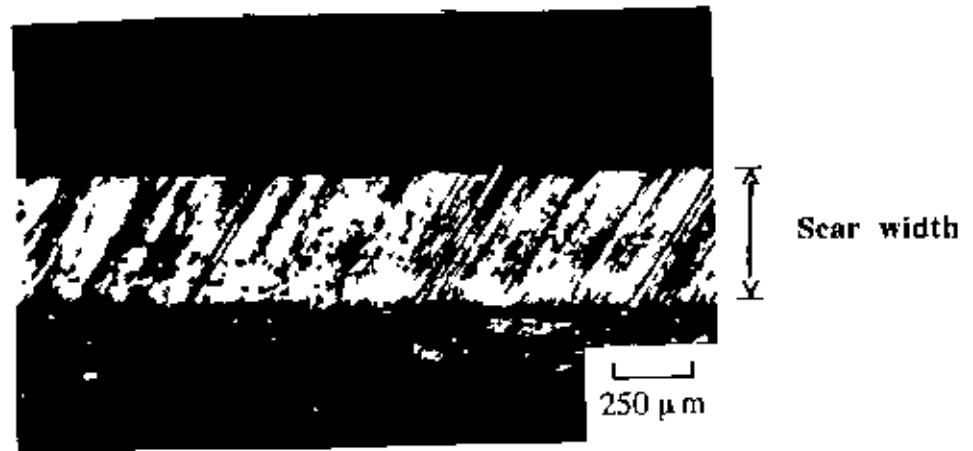
* Deposition current density: 60 mA/cm²

** Deposition current density: 100 mA/cm²

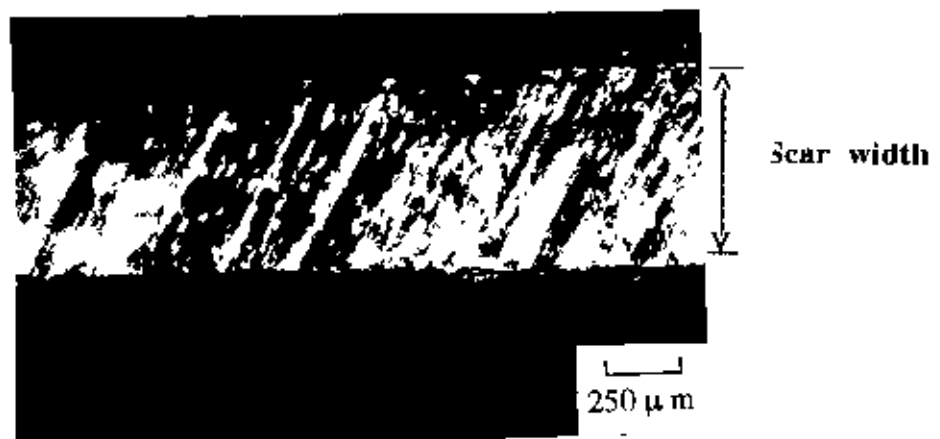
4.3 WEAR BEHAVIOUR

20 μm thick Ni-P coatings deposited on brass pins at current densities of 60 and 100 mA/cm² were investigated for their wear behaviour. Brass pins without coating were also tested for comparison. Wear tests were carried out under three different loads viz, 480, 250 and 180 g for three sliding distances viz, 416 m, 832 m and 1248 m. Earlier studies [44, 45] have established that width of wear scar on coated pin can be taken as a good measure of the extent of wear damage. In the present work also, the extent of wear damage is expressed in terms of width of wear scar.

Figures 4.7 and 4.8 show the micrographs of wear scar on Ni-P alloy coatings deposited at current densities 60 mA/cm² and 100 mA/cm² respectively, and tested under a load of 250 g for different sliding distances. The micrographs were taken immediately after the test without any cleaning. It is seen that the width of wear scar increases with an increase of sliding distance.

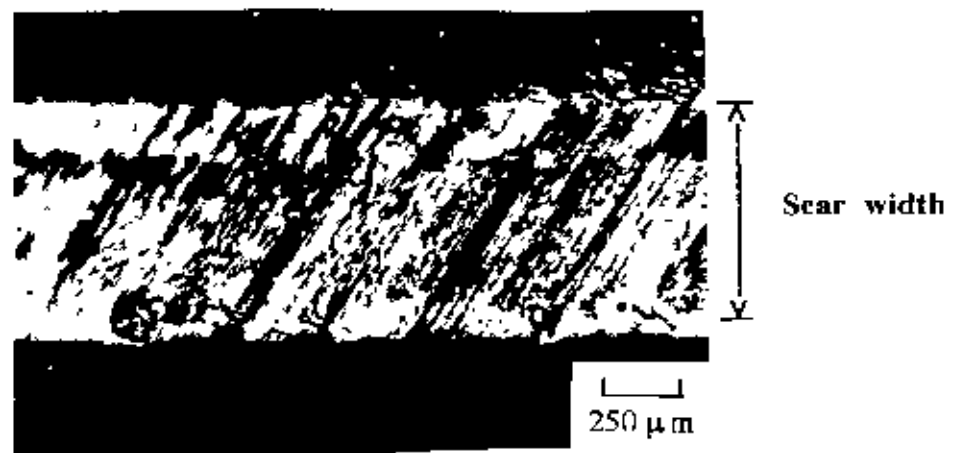


(a)



(b)

Fig. 4.7 Micrographs of wear scar of Ni-P coatings deposited at current density of 60 mA/cm^2 (a) sliding distance 416 m (b) sliding distance 832 m (applied load: 250 gm)



(c)

Fig. 4.7 (continued) (c) sliding distance 1248 m (applied load: 250 gm)

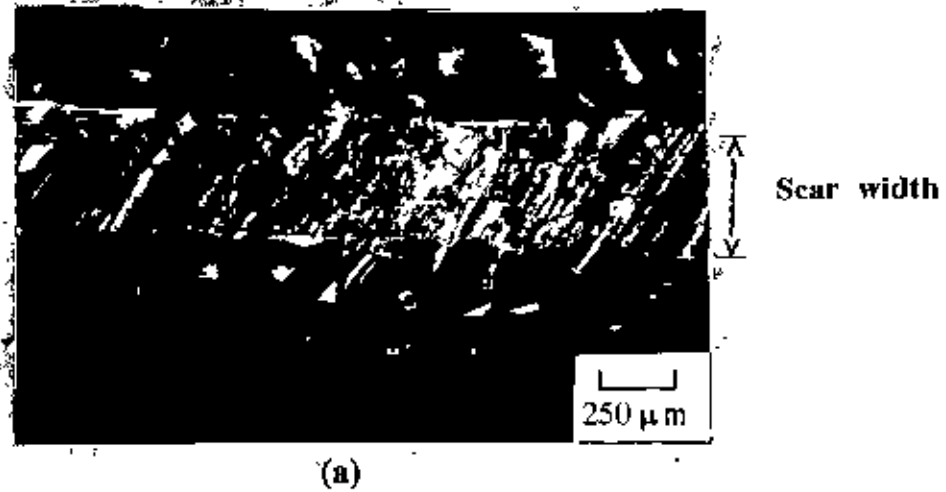


Fig. 4.8 Micrographs of wear scar of Ni-P coatings at current density of 100 mA/cm² (a) sliding distance 416 m (applied load: 250 gm)

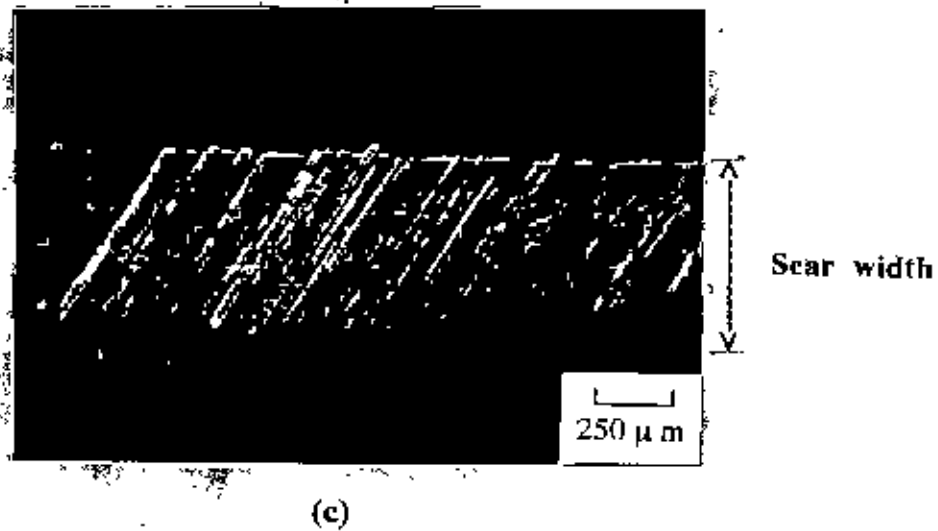
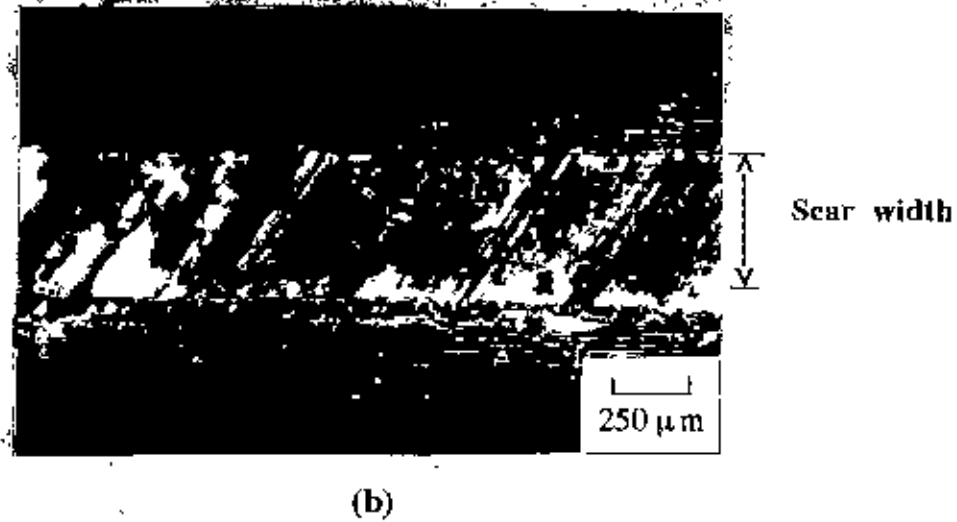


Fig. 4.8 (continued) (b) sliding distance 832 m and (c) sliding distance 1248 (applied load: 250 gm)

The variation of width of wear scar as a function of sliding distance at various loads is shown in Fig. 4.9-4.11. It is seen from Fig. 4.10 that maximum wear damage is sustained by uncoated brass specimens. Nickel-phosphorus coatings deposited at 60 and 100 mA/cm² are found to possess considerable resistance to wear. The wear damage on coatings electrodeposited at 60 mA/cm² is slightly more than that of specimens electrodeposited at 100 mA/cm². From Fig. 4.10, it is evident that the wear scar width on uncoated sample is about four times the wear scar width on coated samples.

From Figs. 4.9-4.11, it is seen that the rate of increase of the wear scar width of both coated samples (at 60 and 100 mA/cm²) is higher at shorter sliding distance but they tend to get reduced at higher sliding distance.

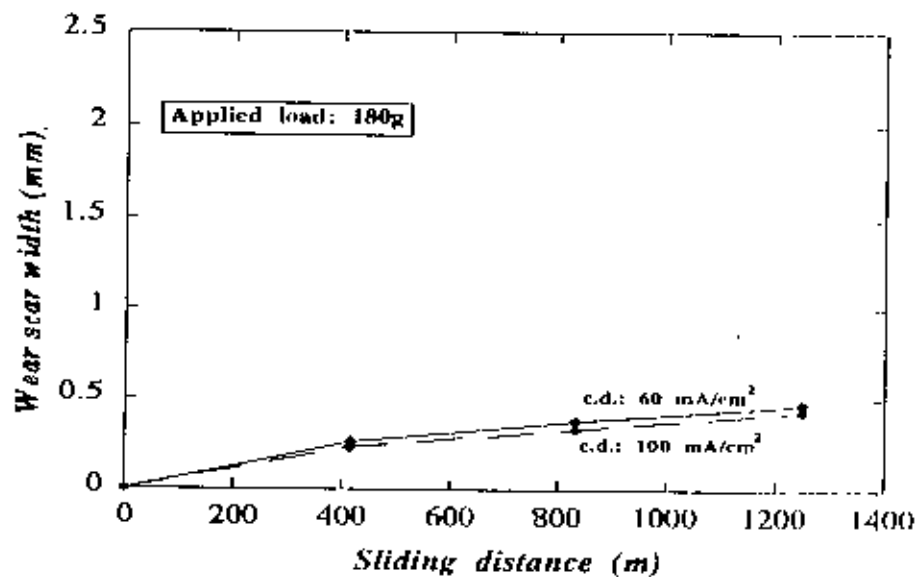


Fig. 4.9 Variation of wear scar width as a function of sliding distance (applied load: 180 g).

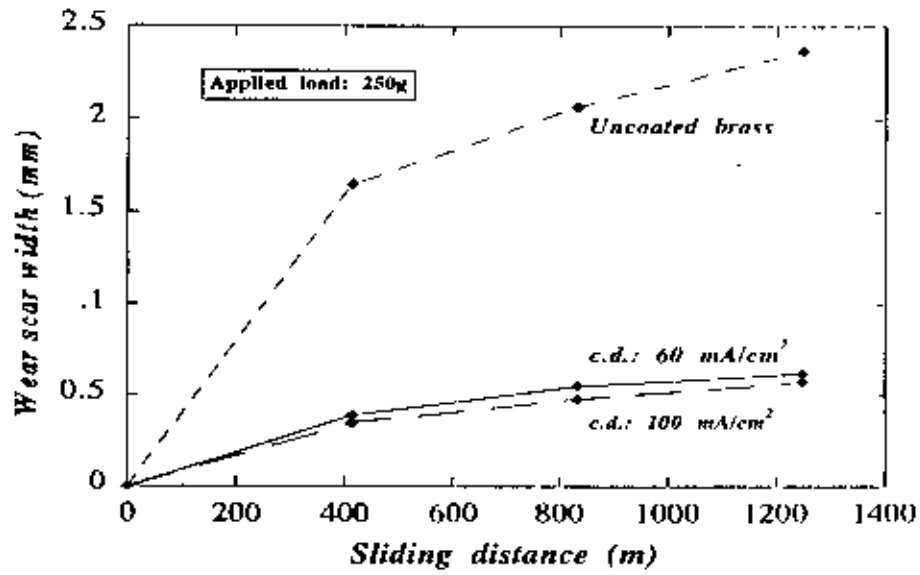


Fig. 4.10 Variation of wear scar width as a function of sliding distance (applied load: 250 g).

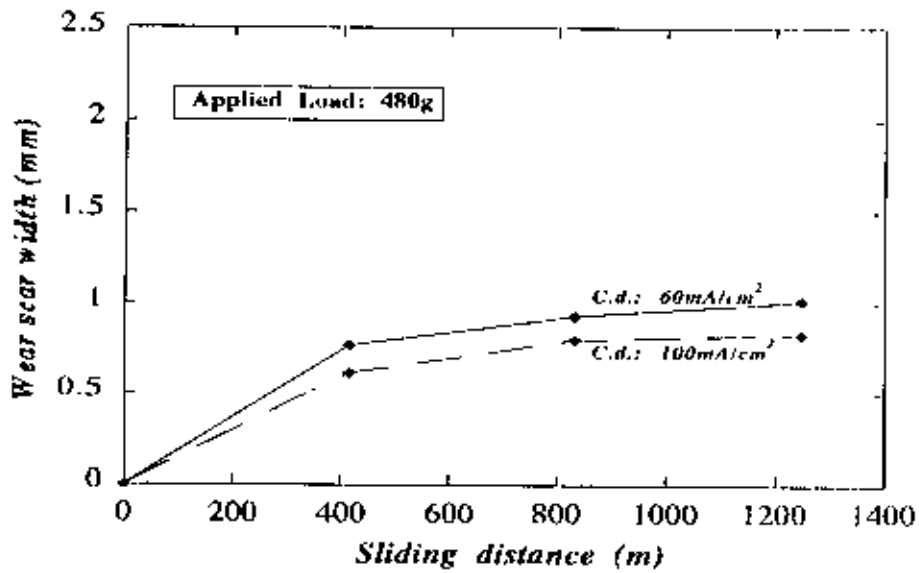


Fig. 4.11 Variation of wear scar width as a function of sliding distance (applied load: 480 g).

Figs. 4.12-4.14 show the variation of wear scar width as a function of applied load at various sliding distances. Wear damage is found to increase more or less steadily as load increases. Coatings deposited at 100 mA/cm^2 is found to be more resistant to wear than coatings deposited at 60 mA/cm^2 . Moreover as the load increases, Ni-P coatings deposited at 100 mA/cm^2 is found to be increasingly more resistant to wear as compared with samples deposited at 60 mA/cm^2 when applied load increases.

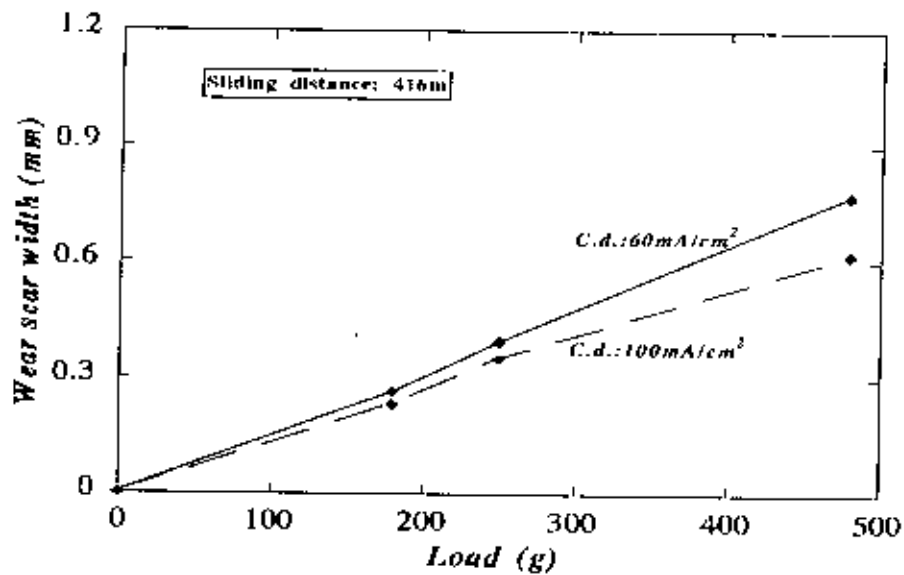


Fig. 4.12 Variation of wear scar width as a function of applied load (sliding distance : 416 m)

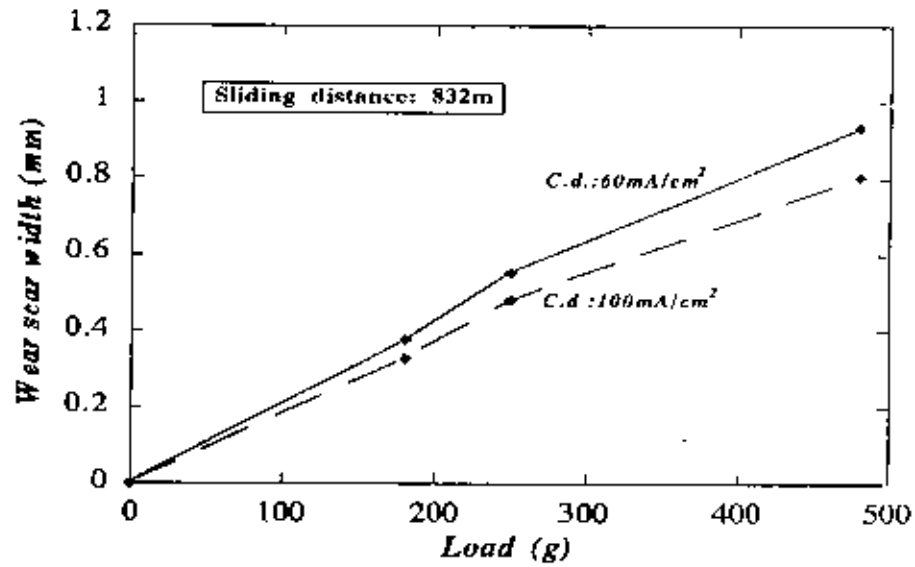


Fig. 4.13 Variation of wear scar width as a function of applied load (sliding distance: 832 m).

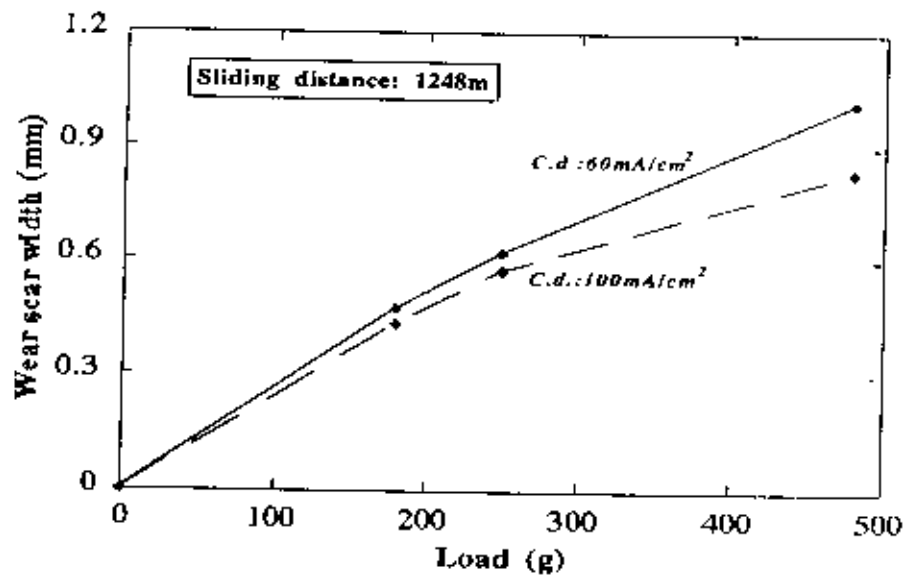
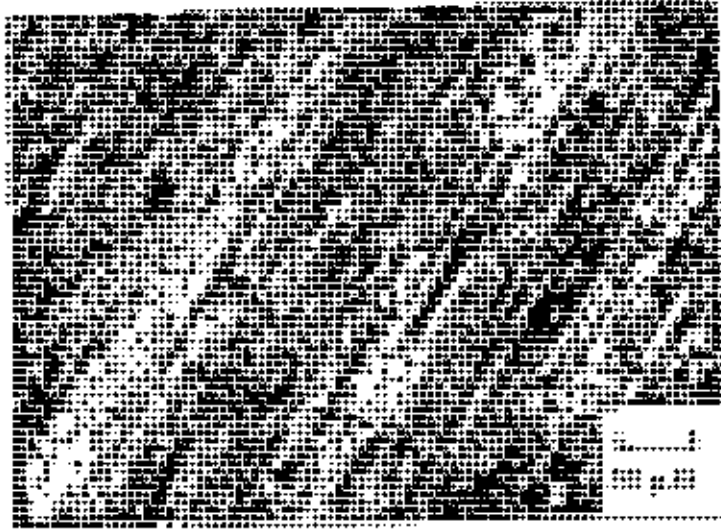


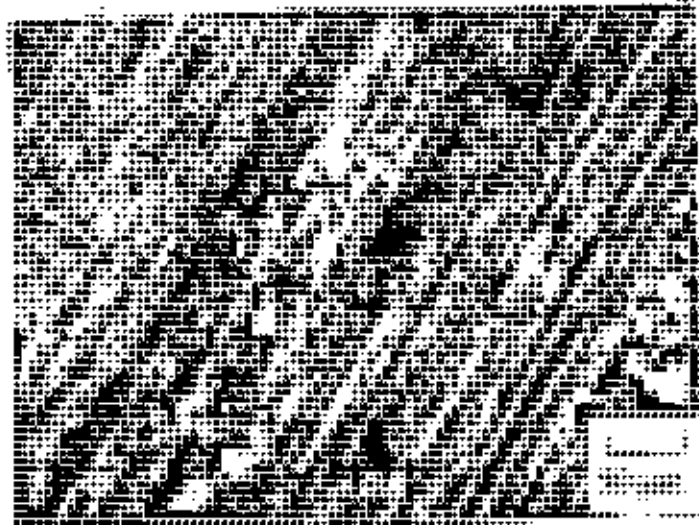
Fig. 4.14 Variation of wear scar width as a function of applied load (sliding distance: 1248 m).

The photomicrographs of wear scars on Ni-P alloy coatings are shown in Fig. 4.15. All the micrographs were taken without any cleaning of the scars. The worn surface of Ni-P coatings mainly consists of relatively fine sliding marks. In addition, small patches of debris are seen scattered on the surface. The sliding marks are believed to have caused by asperities of the counter body and/or hardened debris through microcutting and microploughing action. Such type of micromechanism leads to what is known as abrasive wear. Furthermore, patches of debris on the worn surface of Ni-P coatings are likely to be a transfer layer from cast iron counter body. Haseeb [43] has shown that transfer of iron from steel counter body to nickel surface takes place due to strong chemical interaction between nickel and iron. However, the extent of transfer of iron and hence the thickness of transfer layer on Ni-P coatings in the present case are much lower than those on nickel described by Haseeb. This is due to higher hardness of Ni-P coatings. It is concluded that on Ni-P coatings wear take place mainly by abrasion of asperities on counter body and/or fine hardened debris particles. Some adhesive type of wear also takes place. Sometimes microcracking was found on Ni-P deposits (Fig 4.16). It is thought that these cracks were caused by insufficient support provided by the relatively weak brass substrate to the applied load during testing.

The micrograph of wear scars on uncoated brass is shown in Fig. 4.17. The micrograph was taken without any cleaning of the scar. The wear scar on uncoated brass pin is much more rough than the scars on Ni-P coatings (compare Figs. 15 and 17). The grooves on the scar on brass are much deeper. Evidences of plastic deformation is visible on the scar. The uncoated brass has clearly suffered much more damage than Ni-P coated brass. Little transfer layer or debris is seen. Microploughing by relatively hard asperities on cast iron counter body is suggested to be the main wear mechanism.



(a)



(b)

Fig. 4.15 Micrographs of wear scar of Ni-P coatings (a) deposition current density 60 mA/cm^2 , and (b) deposition current density 100 mA/cm^2 (applied load: 250 gm , sliding distance: 1248 m).

CHAPTER: FIVE

5. CONCLUSIONS

5.1 CONCLUSIONS DRAWN FROM THE PRESENT WORK

1. Hypophosphite based bath containing 100 g/l of sodium hypophosphite was found to yield bright, adherent and hard (665-701) deposit.
2. Ni-P coatings deposited at current densities of 60-200 mA/cm² were found to contain about 14 wt.% phosphorous and all were found to be amorphous.
3. Thickness of Ni-P coatings was found to increase with an increases in current density and deposition time but decrease with the amount of sodium hypophosphite in plating bath.
4. Ni-P coating deposited at a current density of 100 mA/cm² was slightly more wear resistant than the coating deposited at 60 mA/cm². Ni-P coated specimens were found to be about four times more wear resistant than uncoated brass specimen.

5.2 SUGGESTIONS FOR FURTHER WORK

1. Microhardness and wear behaviour of Ni-P coatings should be carried out in the heat-treated condition.
2. X-ray diffraction studies should be carried out on heat-treated Ni-P coatings to understand the phase changes.
3. Other properties, especially magnetic properties and corrosion resistance of Ni-P coatings should be investigated.
4. Dependence of wear behaviour of Ni-P coatings on deposition current density should be studied in detail.

6. REFERENCES

- [1] J. Wurtz, *Comptes Rendus*, 21 (1845) 139-155.
- [2] F.A. Roux, *Us Patent*, 1 (1916) 207, 218.
- [3] A. Brenner and G.F. Riddell, *J. Research National Bur Sandards*, 39 (1947) 385-395.
- [4] A. Brenner D.E. Couch and E.K. Williams, *Electrodeposition of alloys of phosphorus with nickel or cobalt*, *J. Research Natl. Bur standards*, 44 (1950) 109.
- [5] R.B. Diegle, N.R. Sorensen and G.C. Nelson, *J. Electrochem.Soc.*, 133 (1985) 1769.
- [6] D.A. Luke, *Trans. Inst. Metal Finish.*, 64 (1986) 99.
- [7] R. Schloegl, in *Rapidly Quenched Metals*, Elsevier science Publishers B.V., 1985.
- [8] E. Vafaci-Makhsos, E.L. Thomas and L.E. Toth, *Metall. Trans. A*, 9 (1978) 1449
- [9] H. Bestgen, *Ph. D. Thesis*, Universitat Koln, 1984.
- [10] K. Huller and G. Dietz, *J. Magn. Magn. Mater.*, 50 (1985) 250.
- [11] I. Bakonyi, A. Cziraki, I. Nagy and M. Hosso, *Z. Metallkd.*, 77 (1986) 425.
- [12] I. Bakonyi, in *Proc. 5th Int. Seminar on Magnetism*, Berggiesshubel, 1984, *Wiss. Z. Hochschule fur Verkehrswesen Dresden, Sonderheft 13* (1984) 161.

89407

- [13] A. Brenner "Electrodeposition of Alloys" vol.I Academic press N.Y. (1963).
- [14] Jose L. Carbajal and Ralph E. White, *J. Electrochem. Soc.*, 135 (1988) 2955.
- [15] R. Narayan and M.N. Mungole, *Surf. Tech.*, 24 (1985) 235.
- [16] M. Raizker, D.S. Lashmore and K.W. Patt, *Plat. Surf. Finish.*, 73 (1986) 75-80.
- [17] Tohru Watanabe and Takanori Kanayaya, Process of Amorphous in electroplated Ni-P alloy, *J. Surf. Finish. Soc. Jpn.*, 40 (1989) 425.
- [18] I Atanasiu, A. Calusaruc and M. Popescu, Contribution to the study of the electrolytic production of nickel-phosphorus alloys. *Rev. Chim*, 1 (1958) 8-13.
- [19] E. Bredael, J.P. Cclis, J.R. Roos, *Surf. and Coat. Tech.*, 58 (1993) 63.
- [20] A. Brenner "Electrodeposition of Alloys" vol. II Academic press, N.Y. (1963).
- [21] J.K. Taylor, Unpublished data, National Bureau of Standards, (1953) 953.
- [22] D.S.Lashmore, and J.F.Weinroth, *Plating surf. Finish.* 63 (1982) 72.
- [23] Ng. P.K., Snyder, D.D., Lasala, *J. Electrochem. Soc.* 135 (1988) 1276.
- [24] I. Atanasiu, A. Calusaru and M. Popescu, Cathodic polarization in baths used for electrodeposition of Ni-P alloys, *Acad. rep.populare Romine, Studii Cercetri Chem*, 6 (1958) 585-596.

- [25] M.E. Goldstein, Electrodeposition of a durable alloy of nickel-phosphorus, *Plating* 46 (1959) 262.
- [26] C. Rajagopal, D. Mukherjee and K.S. Rajagopalan, Amorphous Ni-P alloys on mild steel, *Metal Finish.*, 82 (1984) 59-65.
- [27] Gas Husheng, Gu Haicheng and Zhou Huiju, "Sliding wear and fretting fatigue resistance of amorphous Ni-P coating" 142 (1991) 291-301.
- [28] V.M. Zhogina and B.Ya. Kaznachei, Electrodeposition of magnetic alloys. *Trudy chetvertogo Soveshchaniya Po Elektrokhim.*, Moscow, 1956 (1959) 506-511.
- [29] H. Nowotny and E. Henglein, *Z. Physik. chem.*, 40 (1938) 281.
- [30] A.W. Ruff and D.S. Lashmore, Selection and use of wear Tests for coating, ASTM STP 769, (ed) R.G. Bayer, (1982) 134.
- [31] C.H. DeMinjer and A. Brenner, Further studies of electroless nickel, *Plating*, 44 (1957) 1297-1305.
- [32] B.G. Bagley and D.Turnbull, *Acta Metallurgica*, 18 (1970) 857.
- [33] L.C.Cheu and F.Spacpcu, *Nature*, 336 (1988) 366.
- [34] A.H.Graham, R.W.Lindsay and H.J.Read, *Journal of the electrochemistry society*, 4 (1965) 401.
- [35] E. Toth-Kadar, I. Bakonyi, A. Solyom, J. Hering, G. Konczos, F. Pavlyak, *Surf. coat. Technol.*, 31 (1987) 31.

- [36] A. Kawashima, Y.P. Lu, H. Habazaki, K. Asami, K. Hashimoto, Corrosion Eng., 38 (1989) 643.
- [37] L.M. Goldman, Ph. D. Thesis, Harvard University, Cambridge, 1990.
- [38] T. Omi, S. Kokunai, H. Yamamoto, Trans. JIM, 17 (1976) 370.
- [39] L. Bennett, H.E. Schone and P.S. Gustafson, Phys. Rev. B, 18 (1978) 2027.
- [40] C. Fan, J.P. Celis and J.R. Roos, J. Electrochem. Soc., 138 (1991) 2917.
- [41] A.W. Goldenstein, W. Rostoker, F. Schossberger and G. Gutzzeit J. Electrochem. Soc., 104 (1957) 104.
- [42] A.S.M.A. Haseeb, P. Chakraborty, I. Ahmed, F. caccavale and R. Bertoncello, Thin solid Films, 1995 (in press).
- [43] A.S.M.A. Haseeb, Ph. D. Thesis, Katholickc University of Leuven, Belgium 1992.
- [44] M. Moniruzzam, M.Sc. Engg. Thesis, Dept. of metallurgical Engg., Bangladesh University of Engineering and Technology, Dhaka, 1995.
- [45] A. Yasmin, M.Sc. Engg. Thesis, Dept. of Metallurgical Engg. Bangladesh university of Engineering and Technology, Dhaka, 1995.

